NASA TECHNICAL NOTE

NASA TN D-8399

NASA TN D-8399

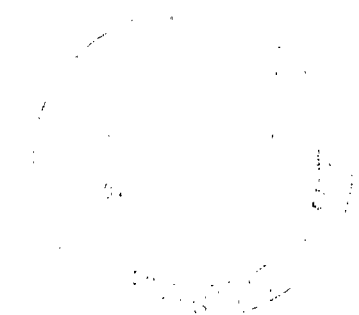# SIMPLIFIED METHODS FOR CALCULATING PHOTODISSOCIATION RATES OF VARIOUS MOLECULES IN SCHUMANN-RUNGE BAND SYSTEMS IN THE UPPER ATMOSPHERE

Tatsuo Shimazaki, Toshihiro Ogawa, and B. C. Farrell

Ames Research Center
Moffett Field, Calif. 94035

NATIONAL AERONAUTICS AND SPACE ADMINISTRATION • WASHINGTON, D. C. • MARCH 1977

0134126

1. Report No. NASA TN D-8399	2. Government Accession No.	3. Recipient's Catalog No.
4. Title and Subtitle SIMPLIFIED METHODS FOR CALCULATING PHOTODISSOCIATION RATES OF VARIOUS MOLECULES IN SCHUMANN-RUNGE BAND SYSTEMS IN THE UPPER ATMOSPHERE		5. Report Date March 1977
		6. Performing Organization Code
7. Author(s) Tatsuo Shimazaki,* Toshihiro Ogawa,† and B. C. Farrell‡		8. Performing Organization Report No. A-6811
		10. Work Unit No. 197-30-02
9. Performing Organization Name and Address *Ames Research Center, Moffett Field, Calif. 94035 †Geophysical Research Laboratory, University of Tokyo, Japan ‡Informatics, Inc., Palo Alto, Calif. 94303		11. Contract or Grant No.
		13. Type of Report and Period Covered Technical Note
12. Sponsoring Agency Name and Address National Aeronautics and Space Administration Washington, D.C. 20546		14. Sponsoring Agency Code

15. Supplementary Notes

16. Abstract

Simplified methods proposed by Hudson and Mahle, and Kockarts for calculating the transmission of solar UV radiation and the dissociation coefficients of various molecules in the Schumann-Runge band spectral region are compared. A significant difference sometimes appears in calculations of the individual band, but the total transmission and the total dissociation coefficients integrated over the entire SR band region agree well between the two methods. The ambiguities in the solar flux data affect the calculated dissociation coefficients more strongly than does the method. A simpler method is developed for the purpose of reducing the computation time and computer memory size necessary for storing coefficients of the equations. The new method can reduce the computation time by a factor of more than 3 and the memory size by a factor of more than 50 compared with the Hudson-Mahle method, and yet the result agrees within 10 percent (in most cases much less) with the original Hudson-Mahle result, except for H_2O and CO_2. A revised method is necessary for these two molecules, whose absorption cross sections change very rapidly over the SR band spectral range.

17. Key Words (Suggested by Author(s)) Photolysis Schumann-Runge band system Upper atmosphere	18. Distribution Statement Unlimited STAR Category — 46		
19. Security Classif. (of this report) Unclassified	20. Security Classif. (of this page) Unclassified	21. No. of Pages 40	22. Price* $3.75

SIMPLIFIED METHODS FOR CALCULATING PHOTODISSOCIATION RATES OF VARIOUS

MOLECULES IN SCHUMANN-RUNGE BAND SYSTEMS IN THE UPPER ATMOSPHERE

Tatsuo Shimazaki, Toshihiro Ogawa,* and B. C. Farrell**

Ames Research Center

SUMMARY

Simplified methods proposed by Hudson and Mahle, and Kockarts for calculating the transmission of solar UV radiation and the dissociation coefficients of various molecules in the Schumann-Runge band spectral region are compared. A significant difference sometimes appears in calculations of the individual band, but the total transmission and the total dissociation coefficients integrated over the entire SR band region agree well between the two methods. The ambiguities in the solar flux data affect the calculated dissociation coefficients more strongly than does the method. A simpler method is developed for the purpose reducing the computation time and computer memory size necessary for storing coefficients of the equations. The new method can reduce the computation time by a factor of more than 3 and the memory size by a factor of more than 50 compared with the Hudson-Mahle method, and yet the result agrees within 10 percent (in most cases much less) with the original Hudson-Mahle result, except for H_2O and CO_2. A revised method is necessary for these two molecules, whose absorption cross sections change very rapidly over the SR band spectral range.

INTRODUCTION

The Schumann-Runge band system of molecular oxygen absorbs solar radiation in the wavelength range of 1750-2050 Å. The main transition occurs between the vibrational levels of $B\ ^3\Sigma_u^-$ (v' = 0, 1, 2, ..., or 19) and of $X\ ^3\Sigma_g^-$ (v'' = 0 or 1). This band system is the main absorber of solar UV radiation in the mesosphere, and various molecules can be photodissociated in these wavelengths in the mesosphere, lower thermosphere, and stratosphere.

Calculations of dissociation rates in Schumann-Runge band wavelengths are necessary in numerical modeling of minor constituent distributions in the upper atmosphere. Because of the very large variability of the O_2 absorption cross section with wavelength and with temperature, exact calculations of radiation transmission and molecular dissociation in the Schumann-Runge bands are complicated and time consuming.

---

 *Geophysical Research Laboratory, University of Tokyo, Japan
**Informatics, Inc., Palo Alto, California 94303

Several methods are described in the literature for calculating the dissociation coefficients at Schumann-Runge band wavelengths by simple analytical formulae. Hudson and Mahle (refs. 1 and 2) and Kockarts (ref. 3) for example, have formulated the results of their elaborate band-to-band calculations based on their data sources into such formulae. In this report we compare the results calculated by these two methods. The main purpose of this report, however, is to present the details of a method that is simpler than previous methods in terms of economy of computer time and computer memory size necessary to store the coefficients appearing in the equations. This method was originally developed and used by Shimazaki and Ogawa (refs. 4 and 5) in their model calculations. In the present report, we demonstrate and discuss the accuracy of this method for duplicating the results obtained with the original Hudson and Mahle method.

GENERAL EQUATIONS

The dissociation coefficient of the ith constituent, at wavelength λ and height z, can be calculated from the expression

$$J_i(\lambda,z) = \sigma_i(\lambda)I_\infty(\lambda)e^{-\tau(\lambda,z)} \tag{1}$$

where σ_i is the absorption cross section of the ith constituent, I_∞ is the intensity of the solar radiation flux at the top of the atmosphere, and τ is the optical depth given by

$$\tau(\lambda,z) = \sum_j \sigma_j(\lambda) \int_z^\infty [X_j]dz \sec \chi \tag{2}$$

where $[X_j]$ denotes the number density of the constituent X_j, and χ is the solar zenith angle. The summation in equation (2) should include all constituents that contribute to absorption at wavelength λ, but it is sufficient in the case of the Earth's upper atmosphere to consider just O_2 and O_3; for other molecules, either $[X_j]$ or σ_j are much smaller. Thus, equation (2) can be simplified as

$$\tau(\lambda,z) = \left[\sigma_{O_2}(\lambda) \int_z^\infty [O_2]dz + \sigma_{O_3}(\lambda) \int_z^\infty [O_3]dz\right] \sec \chi \tag{3}$$

The first and the second terms on the right hand side of equation (3) will be denoted by τ_{O_2} and τ_{O_2}, respectively.

In order to calculate the integrated dissociation coefficient over an entire wavelength region $(\lambda_0 - \lambda_T)$, we divide it into a number of intervals $(\lambda_0 - \lambda_1, \lambda_1 - \lambda_2, \ldots, \lambda_{T-1} - \lambda_T)$. This division could represent either each band or the equally divided interval in the Schumann-Runge band region. Then the total dissociation coefficient can be calculated by

$$J_i(z) = \int_{\lambda_0}^{\lambda_T} J_i(\lambda,z)d\lambda = \sum_{k=0}^{T-1} \int_{\lambda_k}^{\lambda_{k+1}} I_\infty(\lambda)\sigma_i(\lambda)e^{-\tau_{O_2}(\lambda,z)-\tau_{O_3}(\lambda,z)} d\lambda \qquad (4)$$

Assuming that $I_\infty(\lambda)$ and $\tau_{O_3}(\lambda,z)$ are slowly varying functions of λ, we can write the integral in equation (4) as follows:

$$I_k = \overline{I_\infty(\lambda_k)}e^{-\overline{\tau_{O_3}(\lambda_k)}} \int_{\lambda_k}^{\lambda_{k+1}} \sigma_i(\lambda)e^{-\tau_{O_2}(\lambda,z)} d\lambda \qquad (5)$$

where the upper bar indicates the average over the wavelength interval defined by λ_k and λ_{k+1}.

The quantity σ_{O_2}, and therefore τ_{O_2}, is a strong function of λ in the wavelengths of Schumann-Runge band system and thus changes rapidly with λ over the range λ_k to λ_{k+1}. For most constituents other than O_2, σ_i is generally a slowly changing function of λ, and the integral in equation (5) can be simplified using the averaged σ_i over the range of λ_k to λ_{k+1} (see later discussions for the exceptional cases of H_2O and CO_2). Thus, we need two different kinds of integrals to calculate the dissociation rates of molecules in the Schumann-Runge region; that is

$$P(\lambda_k,z)\Delta\lambda_k = \int_{\lambda_k}^{\lambda_{k+1}} e^{-\tau_{O_2}(\lambda,z)} d\lambda \qquad (6)$$

and

$$R(\lambda_k,z)\Delta\lambda_k = \int_{\lambda_k}^{\lambda_{k+1}} \sigma_{O_2}(\lambda)e^{-\tau_{O_2}(\lambda,z)} d\lambda \qquad (7)$$

where $\Delta\lambda_k = \lambda_{k+1} - \lambda_k$.

The former integral (eq. (6)) is called the transmittance of solar radiation and can be used to calculate the total dissociation coefficient of molecules other than O_2 by

$$J_M(z) = \sum_{k=0}^{T-1} \overline{I_\infty(\lambda_k)}\Delta\lambda_k\overline{\sigma_M(\lambda_k)}P(\lambda_k,z)e^{-\overline{\tau_{O_3}(\lambda_k)}} \qquad (8)$$

and the latter integral (eq. (7)) gives the dissociation coefficient for O_2 for unit solar radiation, and can be used to calculate the O_2 dissociation coefficient by

3

$$J_{O_2}(z) = \sum_{k=0}^{T-1} \overline{I_\infty(\lambda_k) \Delta\lambda_k R(\lambda_k,z)} e^{-\overline{\tau_{O_3}(\lambda_k)}} \tag{9}$$

For all molecules, the total dissociation rate is calculated by multiplying the number density of the constituent and the total dissociation coefficient calculated using equations (8) or (9).

NUMERICAL INTEGRATION AND ANALYTICAL APPROXIMATION FORMULAE

Our purpose is to find a simple, effective, and sufficiently accurate method for calculating the integrals P and R given in equations (6) and (7). For this purpose we need to know σ_{O_2} as a function of λ and temperature. We can then evaluate τ_{O_2} as a function of σ_{O_2} and O_2 column density, $N(z)$, which appears in equation (3) as $\int_z^\infty [O_2]dz \sec \chi$.

Experimentally, σ_{O_2} can be evaluated only as an average over the band-width (resolution) of the measuring instrument. Most theoretical calculations assume a Lorentzian line shape for σ_{O_2} given by

$$\sigma_{O_2}(\nu) = \frac{2k_o/\pi\Delta\nu}{1 + \left[\dfrac{2(\nu - \nu_i)}{\Delta\nu}\right]^2} \tag{10}$$

where k_o is the line integrated cross section, ν is the wavenumber in cm^{-1}, ν_i is the wavenumber at the center of a line, and $\Delta\nu$ is the line width. Hudson et al. (ref. 6) have determined two parameters, k_o and $\Delta\nu$, for each band so that the calculated R agrees with the experimental value. Based on k_o and $\Delta\nu$, they have calculated P and R for some chosen values of N in the range of 10^{17} to 7×10^{23} cm^{-2}. The effects of the underlying Schumann-Runge continuum have been incorporated in their calculations. Including the temperature dependence, they have formulated their result as

$$\ln[P(N,T)] = A + B(T - 150) + C(T - 150)^2 \tag{11}$$

and

$$\ln[R(N,T)] = D + E(T - 150) + F(T - 150)^2 \tag{12}$$

for each Schumann-Runge band, except that the bands 19-0, 18-0, and 17-0 are combined into one, and that the band 2-0 is divided into two. The wavelength divisions (19 in number) used in their (ref. 6) calculations are shown as divisions A to S in table 1. The coefficients in equations (11) and (12) are tabulated in reference 3; in each wavelength division, the coefficients A,

B, . . ., F are given for particular chosen values of N. Altogether, there are 5538 coefficients, which must be stored in computer memory in order to use this table in numerical model calculations. Furthermore, in order to calculate P and R for any value of N (or equivalently, height), the necessary coefficients must be obtained by interpolation from the coefficients available in their table. Thus, the Hudson and Mahle method needs a large computer memory for storage and also requires calculation of the necessary coefficients by interpolation.

In an attempt to simplify the numerical procedure, Shimazaki and Ogawa (refs. 4 and 5) have modified the Hudson and Mahle method. Utilizing essentially the same source of data as Hudson and Mahle (ref. 2), Shimazaki and Ogawa derived polynomial formulae of the seventh degree for computing P and R as functions of N:

$$\log P = P_0 + P_1 \log N + P_2 (\log N)^2 + \ldots + P_7 (\log N)^7 \tag{13}$$

and

$$\log R = R_0 + R_1 \log N + R_2 (\log N)^2 + \ldots + R_7 (\log N)^7 \tag{14}$$

Applying this method to each wavelength division of Hudson and Mahle, we have determined the coefficients P_i and R_i by the least square method. The result is shown in tables 2(a) and (b). The effect of the height-dependent temperature is incorporated in these calculations, assuming the temperature profile shown in figure 1. Since the temperature profile in this height range is not expected to change very much, the coefficients tabulated in tables 2(a) and (b) can be used without serious error in most practical cases. This method should give essentially the same result as that of Hudson and Mahle (ref. 2), but the storage requirement is reduced from 5538 to 304 and the interpolation processes can be entirely eliminated. We will refer to this method as SO(1).

In order to further reduce the computation time, Shimazaki and Ogawa (refs. 4 and 5) also changed the wavelength interval from 19 to 6, which divides the Schumann-Runge band region (1750-2050 Å) into equal intervals of 50 Å each. This division into six intervals is shown in table 3 as a part of the partition of the entire spectral range (1350-4000 Å). Above 4000 Å, the atmosphere is almost transparent, although O_3 (Chappuis bands) and NO_2 could absorb slightly at low heights (troposphere). Of 57 wavelength divisions shown in table 3, six divisions with the serial numbers 9 to 14 correspond to the Schumann-Runge band region. For each of these six divisions, the coefficients P_i and R_i have been determined for four temperatures (150, 200, 250, and 300 K) and also for the height-dependent temperatures. The results are tabulated in tables 4 through 8. We refer to this method as SO(2); it needs only 96 coefficients for storage and can reduce the computational time for the Schumann-Runge band region by a factor of about 3 over the method SO(1). We will discuss later the accuracy of the method SO(2) by comparing it with the original Hudson and Mahle method.

Table 3 includes the solar flux and absorption cross section data for the entire spectral range used in model calculations by Shimazaki and Ogawa (refs. 4 and 5) and Ogawa and Shimazaki (ref. 7). These data (except for the Schumann-Runge band region) are used in the present study to calculate the total dissociation coefficient using the Hudson model, and to compare the result with the contribution from the Schumann-Runge bands calculated according to the same model. The partition interval is generally 50 Å except for the spectral range 3100-3300 Å, where the interval 25 Å has been used. The shorter interval is preferable to this range, because the solar spectrum shows a sharp cutoff near 3100 Å and because the quantum yield for $O(^1D)$ production by O_3 photolyses depends upon wavelength.

Ackerman et al. (ref. 8) and Kockarts (ref. 3) calculated P and R for each band assuming a Lorentzian line shape for σ_{O_2} with wavenumber resolution 0.5 cm^{-1}, which is equivalent approximately to a wavelength resolution of 0.02 Å in the Schumann-Runge band region. The values of $\Delta\nu$, determined by these authors on the basis of their experimental data are generally larger than those of Hudson et al. (ref. 6).

The result of elaborate calculations has been used by Kockarts (ref. 3) to construct analytical formula for calculating P and R,

$$\ln R_b(x) = -\alpha \, \exp[c_1(x - x_0) + c_2(x - x_0)^2 + \ldots + c_6(x - x_0)^6] \qquad (15)$$

where R_b stands for either the P and R of the present paper, $x = \ln N$, and the values of x_0, α and c_i are tabulated in his paper for each band. The effect of temperature variation is included in the computation. The method needs 320 memory locations for storage and the computational time is about the same as that for method SO(1), but is about 3 times larger than that of method SO(2).

Kockarts (ref. 3) also determined the coefficients in equation (15) for the constant wavelength interval 10 Å and for the constant wavenumber interval 500 cm^{-1}. The former needs 480 memory locations, and the latter requires 256 locations in order to store the coefficients. The computational time is about 5 and 3 times larger than that of method SO(2) in each case, mainly because of the increased number of divisions.

It should be noted that equation (15) cannot be used for the height range below x_0, which corresponds to about 30 km for the bands of $v' \leq 9$ and to somewhat greater heights for the rest of the bands, because the original integral calculations of P and R were not carried out for these heights.

In table 9 we compare the computer memory size required by the various methods for storing the coefficients and the computation time relative to the method SO(2). Note that the Hudson-Mahle method needs additional time for calculating the coefficients by interpolation.

INPUT DATA

The calculated dissociation coefficients are proportional to the incoming solar radiation flux as is seen in equations (8) and (9). The solar flux values over each wavelength division are listed in table 1 for the Schumann-Runge band region and in table 3 for the entire region of the model calculation. Most models have used the flux values compiled by Ackerman (ref. 9) and we use them for the purpose of comparison among different methods. The recent measurement by Samain and Simon (data taken from Kockarts, ref. 3) indicates much smaller fluxes in the Schumann-Runge band region, and the effect of using those data is calculated using the Kockarts method. Both sets of solar flux data are compared in figure 2.

The absorption cross section spectra of molecules which show appreciable absorption in the Schumann-Runge band region are illustrated in figure 3, and their values for the entire spectral range are listed in table 3.

The ozone density profile, which is needed to calculate τ_{O_3} is taken from observations and is shown in figure 4. This figure also indicates the curves necessary to convert the O_2 column density (N) to the geometrical height. We have shown two curves, one for solar zenith angle 0° (overhead sun) and another for zenith angle 60° (long slant path). The O_2 column density curves are based on the temperature profile shown in figure 1.

RESULTS AND DISCUSSION

For each band, figure 5(a) compares the transmission, and figure 5(b) the O_2 predissociation coefficients, of the Hudson to the Kockarts model. The Kockarts model does not provide values for the region below ~30 km. This may not be a serious limitation for most aeronomically important stratospheric molecules, because H_2O and N_2O are decomposed mainly by chemical reaction with $O(^1D)$ rather than by the photolysis. However, the N_2O photolysis rate could be larger than the chemical reaction rate at heights above ~22 km.

There are significant differences between the two model results as the larger values of N are approached in each band; the Kockarts model generally gives much larger values than the Hudson model. According to Kockarts, the fine resolution used in his method for calculating the integrals P and R generally leads to a larger dissociation rate than the value calculated with the mean absorption cross sections, because the penetration of radiation through the small windows between the absorption lines is allowed. However, the very large difference between the Hudson and Kockarts results, particularly seen in the transitions from larger v' (shorter wavelength region), is more likely to be caused mainly by the effect of the underlying Schumann-Runge continuum, which is included in the Hudson calculation, but not in Kockarts' calculation. The underlying continuum would absorb radiation and result in a smaller transmission and O_2 dissociation rate in the Hudson model than in the Kockarts model.

Near the top of the atmosphere (smaller N) there is a slight, but systematic difference of the O_2 dissociation cross sections between the Hudson and Kockarts models (see fig. 5(b)). The Hudson model tends to give a larger value than the Kockarts model for bands with $v' \geqq 15$, whereas the reverse is the case for the bands with $v' < 14$. The reason for this might be a small but systematic difference of the oscillator strength measured in their experiments, although data are not available in the literature to confirm this. The dissociation coefficient at the top of the atmosphere is related to the absorption oscillator strength (f_{abs}) by

$$\overline{J_\infty(\lambda)} = \frac{\pi e^2}{mc^2} f_{abs}(\lambda)\overline{I_\infty(\lambda)} \tag{16}$$

where m is the electron mass, c the velocity of light, e the electron charge in esu.

In figure 6 the dissociation coefficients of O_2 in the Schumann-Runge bands are compared for three models labeled as Hudson, Kockarts, and Shimazaki. These three are calculated by means of equations (12), (15), and (14) with the coefficients given in Hudson and Mahle (ref. 2), Kockarts (ref. 3), and tables 4 through 8 of the present paper, respectively. In the case of the Shimazaki model, the range calculated for three temperatures (150, 250 and 300 K) is illustrated. The height scale in the abscissa corresponds to the condition of overhead sun.

The total dissociation coefficients of the Hudson model are shown by the uppermost solid curve, whereas the contributions from the Schumann-Runge bands, Schumann-Runge continuum and Herzberg continuum are shown in the lower solid curves. The comparison between the curve for the total and the curve for the Schumann-Runge bands indicates the relative importance of these bands in the height range 70-90 km, above which the Schumann-Runge continuum and below which the Herzberg continuum dominates.

The agreement among methods of the calculated dissociation coefficients in the Schumann-Runge bands is very good, as far as the same solar flux data are used. Most calculations have used the solar fluxes compiled by Ackerman (ref. 9), but the lower dashed curve is calculated for the smaller fluxes observed by Samain and Simon. Comparing this curve with the upper dashed curve calculated for the Ackerman fluxes by the same method, we find that the smaller solar fluxes give appreciably smaller dissociation coefficients; the difference is much larger than the difference caused by the choice of method.

An appreciable temperature effect is seen in Shimazaki's results, as shown in figure 6 for the height range of 80-95 km, where Schumann-Runge band absorption constitutes the major mechanism for O_2 dissociation. At other heights, the temperature effect is relatively small.

The production rates of atomic oxygen from O_2 and O_3 photolyses are shown in figure 7, from which it is seen that the Schumann-Runge bands are the largest source between 80 and 90 km. The result is sensitive to the temperature at these heights, and use of the coefficients corresponding to a lower

temperature (table 5 for 150 K) is essential in order to reproduce, using SO(2), Hudson's result in this height range.

The calculated atomic oxygen production rate has a minimum near 90 km and a maximum near 95 km. It is interesting to note that recent rocket observations (Dickinson et al., ref. 10; Megill et al., ref. 11) indicate a minimum around 94 km and a maximum around 97 km. The height scale in our figures corresponds to an overhead sun; the scale should indicate higher levels for the oblique sun, which was the condition at the time of the rocket observations.

Figures 8(a) through 8(i) compare the dissociation coefficients of various molecules calculated by different methods. If the same solar flux is used, there is good agreement between the Hudson and Kockarts models except for H_2O and CO_2. Except for these two molecules, the absorption cross section does not change very much throughout the Schumann-Runge region (see fig. 3). Since the solar flux increases with increasing wavelengths (see fig. 2), the total dissociation comes mainly from the longer wavelength region (i.e., the transitions of smaller v'). Thus, the large difference of transmission at the shorter wavelength regions (larger v') beween the two models (see fig. 5(b)) does not affect the total dissociation coefficient.

The absorption cross sections of both H_2O and CO_2 decrease rapidly in the Schumann-Runge band region: they decrease by six orders of magnitude for H_2O and four orders of magnitude for CO_2 in the spectral range from 1950 to 2050 Å (see fig. 3). This change is much larger than the corresponding change in the solar flux, which increases about an order of magnitude for the same spectral range. Therefore, the contribution from the shorter wavelength region (or the transitions of larger v') to the total dissociation rate in the Schumann-Runge band region becomes larger. It is in these transitions that the Kockarts model calculates an appreciably larger transmission than the Hudson model (see fig. 5(a)). Thus, the total dissociation rates for H_2O and CO_2 are generally larger in the Kockarts model than in the Hudson model. The magnitude of this difference could be comparable to the difference caused by use of the two different solar spectra for the height region of $N > 10^{21}$ cm^{-2} in the case of H_2O, and of $10^{22} > N > 10^{20}$ cm^{-2} in case of CO_2. At other heights for H_2O and CO_2, and also over the entire height range for other molecules, the effect of changing the solar spectrum is much larger than the effect of using different methods.

Of nine molecules shown in figures 8(a) through 8(i), H_2O dissociation occurs almost exclusively in the Schumann-Runge band region, as does a small fraction (<5 percent) of H_2O_2 dissociation (note the reduction by a factor of 10 for illustrating a total rate curve in fig. 8(f)). For most other molecules, dissociation in Schumann-Runge band system is comparable to dissociation at other parts of the spectral range. As is seen in table 3, HNO_3 and H_2O_2 have appreciable absorption at wavelengths longer than the Schumann-Runge bands, and the contribution from this spectral range becomes dominant as we go to lower heights.

The method SO(2) was derived to reproduce the Hudson model result, but with much less computer time and memory core for storage. In figures 6 and 8,

the results calculated by the method SO(2) are shown by short vertical lines for the range T = 150 to 300 K. A cross on the line indicates the result for T = 250 K. The result generally agress well with the Hudson model result. As is seen in table 10, the difference is generally within 10 percent (in most cases a much smaller percentage) except for H_2O and CO_2, if the coefficients for appropriate temperatures are used. The temperature effect is particularly large in the lower stratosphere (larger N); a larger temperature gives a smaller value, whereas a smaller temperature gives a larger value, for the dissociation coefficient. The difference between two cases of 150 K and 300 K in the lower stratosphere can be as large as 40 percent, whereas the difference in the upper regions is much smaller. The results calculated for the height-dependent temperature using the coefficients in table 8 give the smallest difference for the entire height (or N value) range, although the difference is sometimes larger than the result of constant temperature for some particular value of N. For H_2O and CO_2 the absorption cross sections vary greatly over the 50 Å interval, and the use of the mean cross section in equation (8) would certainly cause a large error.

CONCLUSIONS

The major conclusions that may be drawn from this study are summarized as follows:

1. Except for H_2O and CO_2, calculations by the Hudson-Mahle method and Kockarts method are in good agreement over the whole Schumann-Runge bands, provided that the same solar flux data are used. However, occasionally calculations for each band reveal significant differences between the two models, particularly in the shorter wavelength region (transitions of larger v'), due mainly to effects of the underlying Schumann-Runge continuum that were included in the Hudson model but not in the Kockarts model.

2. Effects of using different solar flux data are generally much larger than effects caused by different methods of calculation. In a model using equally divided intervals, it is essential to sum the solar fluxes at each band within that interval rather than to use the mean solar flux multiplied by the wavelength interval.

3. The temperature effect on the O_2 dissociation coefficients is most pronounced in the mesosphere, whereas the effect is strongest in the stratosphere for other molecules.

4. Method SO(2) provides the most economical method in calculating the photodissociation rates in the Schumann-Runge band region. Except for H_2O and CO_2, calculation by this method yields results which agree within 10 percent (usually much less) with the result of the original Hudson and Mahle method as long as temperature effects are properly taken into account.

5. The absorption cross sections of H_2O and CO_2 change greatly over the Schumann-Runge band region (1750-2050 Å) and even over the 50 Å interval

10

within this region. This causes a large difference between the result calcu-
lated by SO(2) and that by the Hudson method. An improved method has to be
developed for these two constituents.

REFERENCES

1. Hudson, Robert D.; and Mahle, Stephen H.: Photodissociation Rates of Molecular Oxygen in the Mesosphere and Lower Thermosphere. J. Geophys. Res., vol. 77, no. 16, June 1972, pp. 2902-2914.

2. Hudson, R. D.; and Mahle, S. H.: Interpolation Constants for Calculation of Transmittance and Rate of Dissociation of Molecular Oxygen in the Mesosphere and Lower Thermosphere. NASA TM X-58,084, 1972.

3. Kockarts, G.: Absorption and Photodissociation in the Schumann-Runge Bands of Molecular Oxygen in the Terrestrial Atmosphere. Planet. Space Sci., vol. 24, no. 6, 1976, pp. 589-604.

4. Shimazaki, Tatsuo; and Ogawa, Toshihiro: A Theoretical Model of Minor Constituent Distributions in the Stratosphere Including Diurnal Variations. J. Geophys. Res., vol. 79, no. 24, Aug. 1974, pp. 3411-3423.

5. Shimazaki, Tatsuo; and Ogawa, Toshihiro: On the Theoretical Model of Vertical Distributions of Minor Neutral Constituents Concentrations in the Stratosphere. NOAA Tech. Memo., ERL OD-20, May 1974, pp. 1-35.

6. Hudson, R. D.; Carter, V. L.; and Breig, E. L.: Predissociation in the Schumann-Runge Bands System of O_2: Laboratory Measurements and Atmospheric Effects. J. Geophys. Res., vol. 74, no. 16, Aug. 1969, pp. 4079-4086.

7. Ogawa, Toshihiro; and Shimazaki, Tatsuo: Diurnal Variations of Odd Nitrogen and Ionic Densities in the Mesosphere and Lower Thermosphere: Simultaneous Solution of Photochemical-Diffusive Equations. J. Geophys. Res., vol. 80, no. 80, Oct. 1975, pp. 3945-3960.

8. Ackerman, M.; Biaumé, F.; and Kockarts, G.: Absorption Cross Sections of the Schumann-Runge Bands of Molecular Oxygen. Planet. Space Sci., vol. 18, no. 11, Nov. 1970, pp. 1639-1651.

9. Ackerman, M.: Ultraviolet Solar Radiation Related to Mesospheric Processes. Mesospheric Models and Related Experiments, G. Fiocco, ed., D. Reidel Publishing, Dordrecht, Holland, 1971, pp. 149-159.

10. Dickinson, P. H. G.; Bolden, R. C.; and Young, R. A.: Measurement of Atomic Oxygen in the Lower Ionosphere Using a Rocket-Borne Resonance Lamp. Nature, vol. 252, Nov. 1974, pp. 289-291.

11. Megill, L. R.; Howlett, L. C.; Pendleton, W. R.; and Baker, K. D.: Structure Observed in Atomic Oxygen Profiles. Paper presented at American Geophysical Union, Spring Annual Meeting, Washington D. C., April 14, 1976.

TABLE 1.- SCHUMANN-RUNGE BANDS (v' - 0) AND SOLAR FLUXES; THE DIVISION A, B, . . ., S
CORRESPONDS TO THE DIVISIONS IN HUDSON AND MAHLE, (REF. 2)

Division	Band	Wavelength range, Å	$\Delta\lambda$	Solar flux, cm^{-2} sec^{-1}	
				Ackerman (ref. 9)	Samain and Simon
A	19-0	1753.40 — 1755.79	2.39	2.99(10)*	1.50(10)
A	18-0	1755.79 — 1758.94	3.15	4.41(10)	2.10(10)
A	17-0	1758.94 — 1763.20	4.26	6.30(10)	2.81(10)
B	16-0	1763.20 — 1768.60	5.40	8.10(10)	3.84(10)
C	15-0	1768.60 — 1774.60	6.00	9.30(10)	6.40(10)
D	14-0	1774.60 — 1782.60	8.00	1.32(11)	8.38(10)
E	13-0	1782.60 — 1792.60	10.00	1.74(11)	1.26(11)
F	12-0	1792.60 — 1803.60	11.00	2.01(11)	1.56(11)
G	11-0	1803.60 — 1816.40	12.80	2.51(11)	2.08(11)
H	10-0	1816.40 — 1830.60	14.20	3.14(11)	2.91(11)
I	9-0	1830.60 — 1846.20	15.60	3.90(11)	3.13(11)
J	8-0	1846.20 — 1863.40	17.20	4.83(11)	3.42(11)
K	7-0	1863.40 — 1882.20	18.80	5.99(11)	4.98(11)
L	6-0	1882.20 — 1902.40	20.20	7.22(11)	6.02(11)
M	5-0	1902.40 — 1924.00	21.60	8.73(11)	7.58(11)
N	4-0	1924.00 — 1947.00	23.00	1.27(12)	8.15(11)
O	3-0	1947.00 — 1971.80	24.80	1.73(12)	1.22(12)
P	2-0	1971.80 — 1985.00	13.20	9.82(11)	1.38(12)
Q	2-0	1985.00 — 2000.00	15.00	1.15(12)	1.38(12)
R	1-0	2000.00 — 2025.00	25.00	2.01(12)	1.79(12)
S	0-0	2025.00 — 2050.00	25.00	2.32(12)	1.09(12)

*Numeral A(k) should read as A×10^k.

TABLE 2.- COEFFICIENTS TO CALCULATE THE TRANSMITTANCE AND THE O_2 DISSOCIATION RATES IN METHOD SO(1) FOR THE HEIGHT-DEPENDENT TEMPERATURE

(a) Coefficients in equation (13)

Division	P_0	P_1	P_2	P_3	P_4	P_5	P_6	P_7
A	9.64245(5)*	-3.86520(5)	6.63259(4)	-6.31624(3)	3.60544(2)	-1.23373(1)	2.34350(-1)	-1.90650(-3)
B	3.60957(5)	-1.47330(5)	2.57512(4)	-2.49860(3)	1.45356(2)	-5.07029(0)	9.81961(-2)	-8.14599(-4)
C	6.25465(5)	-2.50109(5)	4.28066(4)	-4.06510(3)	2.31343(2)	-7.89027(0)	1.49341(-1)	-1.21015(-3)
D	1.93183(5)	-7.73955(4)	1.32748(4)	-1.26368(3)	7.21101(1)	-2.46683(0)	4.68463(-2)	-3.81011(-4)
E	2.99191(5)	-1.18707(5)	2.01547(4)	-1.89835(3)	1.07134(2)	-3.62283(0)	6.79744(-2)	-5.45934(-4)
F	3.40140(5)	-1.33875(5)	2.25420(4)	-2.10506(3)	1.17750(1)	-3.94555(0)	7.33340(-2)	-5.83283(-4)
G	-1.15218(4)	2.96190(3)	-2.25539(2)	-5.22146(0)	1.80514(0)	-1.12618(-1)	3.08878(-3)	-3.27011(-5)
H	4.88031(4)	-1.94837(4)	3.32989(3)	-3.15830(2)	1.79550(1)	-6.11863(-1)	1.15734(-2)	-9.37435(-5)
I	1.13279(5)	-4.37784(4)	7.23463(3)	-6.62764(2)	3.63540(1)	-1.19410(0)	2.17497(-2)	-1.69489(-4)
J	1.15250(5)	-4.41354(4)	7.22532(3)	-6.55542(2)	3.56034(1)	-1.15768(0)	2.08702(-2)	-1.60947(-4)
K	2.00108(5)	-7.63581(4)	1.24593(4)	-1.12578(3)	6.08593(1)	-1.96856(0)	3.52798(-2)	-2.70266(-4)
L	1.71838(5)	-6.50794(4)	1.05284(4)	-9.43188(2)	5.05355(1)	-1.61951(0)	2.87452(-2)	-2.18007(-4)
M	1.52518(5)	-5.77643(4)	9.34530(3)	-8.37233(2)	4.48605(1)	-1.43771(0)	2.55198(-2)	-1.93557(-4)
N	1.65441(5)	-6.24491(4)	1.00680(4)	-8.98693(2)	4.79711(1)	-1.53133(0)	2.70698(-2)	-2.04434(-4)
O	1.17195(5)	-4.42395(4)	7.13295(3)	-6.36809(2)	3.39998(1)	-1.08567(0)	1.91990(-2)	-1.45060(-4)
P	1.10275(5)	-4.16687(4)	6.72545(3)	-6.01086(2)	3.21294(1)	-1.02718(0)	1.81873(-2)	-1.37594(-4)
Q	1.64614(5)	-6.19277(4)	9.94959(3)	-8.85013(2)	4.70722(1)	-1.49718(0)	2.63681(-2)	-1.98383(-4)
R	1.59108(5)	-5.98622(4)	9.61871(3)	-8.55674(2)	4.55169(1)	-1.44788(0)	2.55030(-2)	-1.91900(-4)
S	1.50431(5)	-5.65992(4)	9.09466(3)	-8.09080(2)	4.30399(1)	-1.36914(0)	2.41172(-2)	-1.81480(-4)

(b) Coefficients in equation (14)

Division	R_0	R_1	R_2	R_3	R_4	R_5	R_6	R_7
A	-2.23178(5)*	8.56837(4)	-1.40281(4)	1.26875(3)	-6.84122(1)	2.19706(0)	-3.88602(-2)	2.91491(-4)
B	-5.37174(5)	2.05232(5)	-3.34300(4)	3.00810(3)	-1.61403(2)	5.16081(0)	-9.09771(-2)	6.81390(-4)
C	5.05218(4)	-2.38634(4)	4.74207(3)	-5.15770(2)	3.32375(1)	-1.27127(0)	2.67574(-2)	-2.39337(-4)
D	2.86001(5)	-1.10136(5)	1.81685(4)	-1.66501(3)	9.15777(1)	-3.02391(0)	5.55211(-2)	-4.37388(-4)
E	3.09553(5)	-1.20294(5)	2.00281(4)	-1.85244(3)	1.02816(2)	-3.42490(0)	6.34065(-2)	-5.03326(-4)
F	7.97225(4)	-3.36020(4)	6.05275(3)	-6.04004(2)	3.60534(1)	-1.28701(0)	2.54360(-2)	-2.14680(-4)
G	-1.79013(5)	6.55222(4)	-1.01929(4)	8.72743(2)	-4.43694(1)	1.33735(0)	-2.20843(-2)	1.53700(-4)
H	-1.05587(5)	3.98373(4)	-6.39757(3)	5.66511(2)	-2.98583(1)	9.36092(-1)	-1.61519(-2)	1.18214(-4)
I	-7.39158(4)	2.69609(4)	-4.17706(3)	3.55897(2)	-1.79889(1)	5.38582(-1)	-8.82599(-3)	6.08976(-5)
J	-5.69086(4)	2.01018(4)	-3.00458(3)	2.45731(2)	-1.18416(1)	3.34809(-1)	-5.10954(-3)	3.21228(-5)
K	1.25324(5)	-4.88466(4)	8.13325(3)	-7.50024(2)	4.13684(1)	-1.36466(0)	2.49293(-2)	-1.94543(-4)
L	1.06603(5)	-4.11253(4)	6.77582(3)	-6.18144(2)	3.37201(1)	-1.09986(0)	1.98607(-2)	-1.53161(-4)
M	1.46641(5)	-5.60523(4)	9.14826(3)	-8.26508(2)	4.46411(1)	-1.44144(0)	2.57640(-2)	-1.96648(-4)
N	2.45343(5)	-9.24469(4)	1.48704(4)	-1.32377(3)	7.04348(1)	-2.24007(0)	3.94300(-2)	-2.96348(-4)
O	1.78028(5)	-6.68633(4)	1.07193(4)	-9.51038(2)	5.04335(1)	-1.59866(0)	2.80486(-2)	-2.10146(-4)
P	1.61656(5)	-6.09003(4)	9.79459(3)	-8.71895(2)	4.63969(1)	-1.47597(0)	2.59912(-2)	-1.95462(-4)
Q	1.84740(5)	-6.93295(4)	1.11064(4)	-9.84724(2)	5.21919(1)	-1.65379(0)	2.90116(-2)	-2.17379(-4)
R	1.60886(5)	-6.05304(4)	9.72364(3)	-8.64714(2)	4.59784(1)	-1.46185(0)	2.57351(-2)	-1.93532(-4)
S	1.52009(5)	-5.71919(4)	9.18791(3)	-8.17159(2)	4.34562(1)	-1.38191(0)	2.43329(-2)	-1.83031(-4)

*Numeral A(k) should read as $A \times 10^k$.

TABLE 3.- THE INTEGRATED SOLAR FLUX AND THE MEAN ABSORPTION CROSS SECTIONS FOR VARIOUS MOLECULES OVER EACH OF 57 WAVELENGTH DIVISIONS IN THE SPECTRUM RANGE OF 1350-4000 Å

Division	Wavelength, Å	Solar flux, cm^{-2} sec^{-1}	Mean absorption cross sections, cm^{-2}										
			O_2	O_3	N_2O	H_2O	H_2O_2	HNO_3	HCl	SO_2	$CFCl_3$	CF_2Cl_2	CO_2
1	1350-1400	1.40(10)*	6.70(-18)	1.60(-17)	4.80(-18)	3.40(-18)	7.80(-18)	0	7.60(-19)	0	3.40(-17)	1.20(-18)	7.00(-19)
2	1400-1450	1.93(10)	1.38(-17)	7.70(-18)	1.08(-18)	8.40(-19)	5.60(-18)	0	1.40(-18)	3.16(-18)	1.30(-17)	3.80(-19)	5.20(-19)
3	1450-1500	3.50(10)	1.43(-17)	5.10(-18)	6.60(-18)	5.10(-19)	4.10(-18)	0	2.20(-18)	4.22(-18)	5.20(-18)	1.90(-19)	6.30(-19)
4	1500-1550	5.50(10)	1.12(-17)	3.90(-18)	1.90(-18)	1.07(-18)	3.60(-18)	0	3.00(-18)	5.62(-18)	3.60(-18)	2.10(-19)	5.20(-19)
5	1550-1600	8.25(10)	7.90(-18)	2.00(-18)	1.02(-19)	2.30(-18)	3.30(-18)	0	3.30(-18)	3.65(-18)	3.50(-18)	2.90(-19)	3.70(-19)
6	1600-1650	1.20(11)	4.80(-18)	1.15(-18)	3.70(-20)	3.60(-18)	3.70(-18)	0	2.70(-18)	1.33(-18)	5.20(-18)	1.80(-19)	1.70(-19)
7	1650-1700	1.98(11)	2.20(-18)	8.30(-19)	5.80(-20)	4.60(-18)	3.90(-18)	7.10(-18)	2.00(-18)	4.22(-19)	6.20(-18)	2.00(-19)	7.20(-20)
8	1700-1750	3.60(11)	6.70(-19)	8.10(-19)	9.30(-20)	3.60(-18)	3.20(-18)	9.40(-18)	1.20(-18)	4.87(-19)	5.20(-18)	3.20(-19)	1.30(-20)
9	1750-1800	8.17(11)	1.30(-23)	8.30(-19)	1.34(-19)	1.85(-18)	1.71(-18)	1.29(-17)	6.20(-19)	1.00(-18)	5.00(-18)	4.60(-19)	2.90(-21)
10	1800-1850	1.12(12)	1.31(-23)	6.90(-19)	1.41(-19)	2.20(-18)	1.18(-18)	1.30(-17)	3.60(-19)	1.78(-18)	5.20(-18)	5.40(-19)	5.80(-22)
11	1850-1900	1.61(12)	1.33(-23)	6.00(-19)	1.26(-19)	1.50(-20)	1.05(-18)	1.15(-17)	1.70(-19)	4.22(-18)	2.40(-18)	9.00(-19)	1.35(-22)
12	1900-1950	2.43(12)	1.31(-23)	4.50(-19)	9.70(-20)	1.60(-21)	6.70(-19)	1.13(-17)	9.00(-20)	4.22(-18)	1.90(-18)	6.00(-19)	2.70(-23)
13	1950-2000	3.64(12)	1.25(-23)	3.60(-19)	6.00(-20)	1.75(-22)	5.60(-19)	7.20(-18)	3.60(-20)	3.16(-18)	1.10(-18)	2.40(-19)	8.00(-24)
14	2000-2050	4.33(12)	1.20(-23)	3.05(-19)	2.80(-20)	1.50(-23)	4.90(-19)	3.70(-18)	1.60(-20)	2.37(-18)	6.50(-19)	8.60(-20)	3.70(-24)
15	2050-2100	7.50(12)	1.18(-23)	3.75(-19)	1.48(-20)		4.40(-19)	2.10(-18)	7.20(-21)	1.78(-18)	3.50(-19)	3.10(-20)	3.10(-24)
16	2100-2150	1.63(13)	1.08(-23)	5.30(-19)	7.10(-21)		4.00(-19)	9.70(-19)	3.70(-21)	1.15(-18)	1.60(-19)	1.20(-20)	2.80(-24)
17	2150-2200	2.50(13)	9.30(-24)	9.50(-19)	2.90(-21)		3.40(-19)	3.28(-19)	1.50(-21)	5.62(-19)	6.20(-20)	2.10(-21)	2.20(-24)
18	2200-2250	3.45(13)	7.30(-24)	1.80(-18)	1.15(-21)		2.80(-19)	1.44(-19)		2.37(-19)	2.20(-20)	4.00(-22)	
19	2250-2300	4.15(13)	5.00(-24)	2.90(-18)	4.80(-22)		2.40(-19)	8.51(-20)		1.33(-19)	1.00(-20)		
20	2300-2350	4.40(13)	2.90(-24)	4.40(-18)	5.00(-23)		2.05(-19)	5.63(-20)		2.05(-20)	3.80(-21)		
21	2350-2400	4.00(13)	1.40(-24)	6.20(-18)	2.00(-23)		1.70(-19)	3.74(-20)			1.30(-21)		
22	2400-2450	3.90(13)	3.10(-25)	8.10(-18)	5.00(-24)		1.40(-19)	2.60(-20)					
23	2450-2500	4.25(13)		9.80(-18)	2.00(-24)		1.15(-19)	2.10(-20)					
24	2500-2550	4.75(13)		1.10(-17)	6.00(-25)		1.02(-19)	1.95(-20)					
25	2550-2600	6.00(13)		1.10(-17)	4.00(-25)		8.30(-20)	1.94(-20)					
26	2600-2650	1.00(14)		1.07(-17)	2.50(-25)		6.90(-20)	1.90(-20)					
27	2650-2700	1.50(14)		9.80(-18)	1.00(-25)		5.40(-20)	1.80(-20)					
28	2700-2750	1.85(14)		7.70(-18)			4.10(-20)	1.63(-20)					
29	2750-2800	1.80(14)		5.80(-18)			3.10(-20)	1.40(-20)					
30	2800-2850	1.88(14)		3.80(-18)			2.40(-20)	1.14(-20)					
31	2850-2900	2.50(14)		2.40(-18)			1.90(-20)	8.77(-21)					
32	2900-2950	3.75(14)		1.43(-18)			1.50(-20)	6.34(-21)					
33	2950-3000	4.50(14)		7.50(-19)			1.20(-20)	4.26(-21)					
34	3000-3050	4.50(14)		3.75(-19)			1.00(-20)	2.76(-21)					
35	3050-3100	5.00(14)		1.93(-19)			8.00(-21)	1.68(-21)					
36	3100-3125	2.75(14)		1.28(-19)			7.00(-21)	9.50(-22)					
37	3125-3150	3.13(14)		9.00(-20)			6.45(-21)	7.10(-22)					
38	3150-3175	3.38(14)		6.33(-20)			5.90(-21)	4.70(-22)					
39	3175-3200	3.63(14)		4.75(-20)			5.45(-21)	3.25(-22)					
40	3200-3225	3.88(14)		3.50(-20)			5.00(-21)	1.80(-22)					
41	3225-3250	4.00(14)		2.25(-20)			4.75(-21)	1.00(-22)					
42	3250-3275	4.25(14)		1.80(-20)			4.50(-21)	2.00(-23)					
43	3275-3300	4.38(14)		1.00(-20)			4.25(-21)	1.00(-23)					
44	3300-3350	9.00(14)		6.40(-21)			4.00(-21)						
45	3350-3400	9.25(14)		3.20(-21)			3.50(-21)						
46	3400-3450	9.75(14)		1.47(-21)			3.00(-21)						
47	3450-3500	1.00(15)		6.70(-22)			2.60(-21)						
48	3500-3550	1.03(15)		3.00(-22)			2.20(-21)						
49	3550-3600	1.05(15)		1.30(-22)			1.90(-21)						
50	3600-3650	1.05(15)		4.00(-23)			1.50(-21)						
51	3650-3700	1.18(15)		0.			1.20(-21)						
52	3700-3750	1.23(15)		0.			8.70(-22)						
53	3750-3800	1.23(15)		0.									
54	3800-3850	1.15(15)		0.									
55	3850-3900	1.10(15)		0.									
56	3900-3950	1.10(15)		0.									
57	3950-4000	1.18(15)		0.									

*Numeral A(k) should read as $A \times 10^k$

TABLE 4.- COEFFICIENTS TO CALCULATE THE TRANSMITTANCE AND THE O_2 DISSOCIATION RATES IN METHOD SO(2) FOR THE TEMPERATURE 150 K

	(a) Coefficients in equation (13)							
Division	P_0	P_1	P_2	P_3	P_4	P_5	P_6	P_7
9	1.08163(5)*	-4.36764(4)	7.54442(3)	-7.22630(2)	4.14515(1)	-1.42398(0)	2.71263(-2)	-2.21064(-4)
10	9.90159(4)	-3.86648(4)	6.45620(3)	-5.97597(2)	3.31170(1)	-1.09882(0)	2.02134(-2)	-1.59044(-4)
11	4.14770(4)	-1.59751(4)	2.63012(3)	-2.39958(2)	1.31033(1)	-4.28297(-1)	7.75988(-3)	-6.01254(-5)
12	1.12919(5)	-4.29609(4)	6.98196(3)	-6.28339(2)	3.38191(1)	-1.08868(0)	1.94090(-2)	-1.47841(-4)
13	1.02245(5)	-3.88122(4)	6.29303(3)	-5.64979(2)	3.03337(1)	-9.73997(-1)	1.73191(-2)	-1.31567(-4)
14	1.08779(5)	-4.12757(4)	6.68954(3)	-6.00299(2)	3.22141(1)	-1.03382(0)	1.83724(-2)	-1.39483(-4)

	(b) Coefficients in equation (14)							
Division	R_0	R_1	R_2	R_3	R_4	R_5	R_6	R_7
9	1.49188(5)	-6.10004(4)	1.06590(4)	-1.03181(3)	5.97557(1)	-2.07022(0)	3.97252(-2)	-3.25693(-4)
10	7.59127(3)	-4.04242(3)	8.62047(2)	-9.77888(1)	6.44842(0)	-2.48941(-1)	5.23358(-3)	-4.63733(-5)
11	-1.76776(3)	-3.99100(2)	2.43967(2)	-3.85736(1)	2.99367(0)	-1.26513(-1)	2.80113(-3)	-2.55381(-5)
12	1.54261(5)	-5.90490(4)	9.64901(3)	-8.72585(2)	4.71617(1)	-1.52339(0)	2.72295(-2)	-2.07764(-4)
13	2.01203(5)	-7.60616(4)	1.22747(4)	-1.09628(3)	5.85215(1)	-1.86726(0)	3.29741(-2)	-2.48619(-4)
14	1.20114(5)	-4.55305(4)	7.36960(3)	-6.60406(2)	3.53867(1)	-1.13383(0)	2.01152(-2)	-1.52437(-4)

*Numeral A(k) should read as $A \times 10^k$.

TABLE 5.- COEFFICIENTS TO CALCULATE THE TRANSMITTANCE AND THE O_2 DISSOCIATION RATES IN METHOD SO(2) FOR THE TEMPERATURE 200 K

	(a) Coefficients in equation (13)							
Division	P_0	P_1	P_2	P_3	P_4	P_5	P_6	P_7
9	1.96036(5)*	-7.80681(4)	1.33010(4)	-1.25683(3)	7.11343(1)	-2.41158(0)	4.53451(-2)	-3.64821(-4)
10	1.08986(5)	-4.23452(4)	7.03569(3)	-6.48041(2)	3.57390(1)	-1.18020(0)	2.16101(-2)	-1.69270(-4)
11	1.16123(5)	-4.40549(4)	7.14072(3)	-6.41050(2)	3.44268(1)	-1.10609(0)	1.96874(-2)	-1.49773(-4)
12	1.36331(5)	-5.16006(4)	8.34279(3)	-7.46943(2)	3.99972(1)	-1.28104(0)	2.27241(-2)	-1.72240(-4)
13	1.98379(5)	-7.45194(4)	1.19541(4)	-1.06161(3)	5.63704(1)	-1.78980(0)	3.14651(-2)	-2.36292(-4)
14	1.53176(5)	-5.76353(4)	9.26175(3)	-8.24002(2)	4.38367(1)	-1.39459(0)	2.45673(-2)	-1.84881(-4)

	(b) Coefficients in equation (14)							
Division	R_0	R_1	R_2	R_3	R_4	R_5	R_6	R_7
9	2.12571(5)	-8.57646(4)	1.47986(4)	-1.41561(3)	8.10690(1)	-2.77918(0)	5.28044(-2)	-4.28929(-4)
10	-1.55042(4)	4.83256(3)	-5.95733(2)	3.49003(1)	-7.80037(-1)	-1.32515(-2)	9.74658(-4)	-1.34721(-5)
11	8.03231(3)	-4.11842(3)	8.45482(2)	-9.23056(1)	5.85665(0)	-2.17503(-1)	4.39831(-3)	-3.74845(-5)
12	1.87325(5)	-7.11816(4)	1.15484(4)	-1.03706(3)	5.56698(1)	-1.78636(0)	3.17269(-2)	-2.40602(-4)
13	2.51679(5)	-9.44945(4)	1.51462(4)	-1.34366(3)	7.12527(1)	-2.25866(0)	3.96309(-2)	-2.96941(-4)
14	1.52335(5)	-5.73294(4)	9.21296(3)	-8.19702(2)	4.36107(1)	-1.38750(0)	2.44446(-2)	-1.83976(-4)

*Numeral A(k) should read as $A \times 10^k$.

TABLE 6.- COEFFICIENTS TO CALCULATE THE TRANSMITTANCE AND THE O_2 DISSOCIATION RATES IN METHOD SO(2) FOR THE TEMPERATURE 250 K

(a) Coefficients in equation (13)

Division	P_0	P_1	P_2	P_3	P_4	P_5	P_6	P_7
9	1.73786(5)*	-6.95971(4)	1.19236(4)	-1.13285(3)	6.44629(1)	-2.19698(0)	4.15251(-2)	-3.35795(-4)
10	1.24912(5)	-4.85446(4)	8.06623(3)	-7.42874(2)	4.09564(1)	-1.35182(0)	2.47353(-2)	-1.93577(-4)
11	6.50601(4)	-2.48561(4)	4.05765(3)	-3.66920(2)	1.98509(1)	-6.42600(-1)	1.15260(-2)	-8.83798(-5)
12	1.08752(5)	-4.13879(4)	6.72861(3)	-6.05778(2)	3.26197(1)	-1.05062(0)	1.87422(-2)	-1.42865(-4)
13	1.01484(5)	-3.85372(4)	6.25082(3)	-5.61420(2)	3.01559(1)	-9.68744(-1)	1.72344(-2)	-1.30995(-4)
14	1.08702(5)	-4.12487(4)	6.68555(3)	-5.99977(2)	3.21990(1)	-1.03341(0)	1.83665(-2)	-1.39450(-4)

(b) Coefficients in equation (14)

Division	R_0	R_1	R_2	R_3	R_4	R_5	R_6	R_7
9	2.03153(5)	-8.26752(4)	1.43801(4)	-1.38579(3)	7.99048(1)	-2.75653(0)	5.26774(-2)	-4.30174(-4)
10	1.27615(4)	-6.08681(3)	1.20471(3)	-1.29348(2)	8.17326(0)	-3.04885(-1)	6.23080(-3)	-5.39116(-5)
11	-3.07120(4)	1.07858(4)	-1.60420(3)	1.30689(2)	-6.28491(0)	1.77891(-1)	-2.73213(-3)	1.74449(-5)
12	1.50342(5)	-5.72943(4)	9.32189(3)	-8.39481(2)	4.51905(1)	-1.45415(0)	2.58985(-2)	-1.96949(-4)
13	1.36436(5)	-5.15881(4)	8.32721(3)	-7.43976(2)	3.97337(1)	-1.26857(0)	2.24189(-2)	-1.69194(-4)
14	9.39704(4)	-3.57067(4)	5.79409(3)	-5.20618(2)	2.79762(1)	-8.99109(-1)	1.60024(-2)	-1.21680(-4)

*Numeral A(k) should read as $A \times 10^k$.

TABLE 7.- COEFFICIENTS TO CALCULATE THE TRANSMITTANCE AND THE O_2 DISSOCIATION RATES IN METHOD SO(2) FOR THE TEMPERATURE 300 K

(a) Coefficients in equation (13)

Division	P_0	P_1	P_2	P_3	P_4	P_5	P_6	P_7
9	1.65842(5)*	-6.67551(4)	1.14943(4)	-1.09747(3)	6.27528(1)	-2.14886(0)	4.08038(-2)	-3.31453(-4)
10	1.48480(5)	-5.75904(4)	9.54942(3)	-8.77549(2)	4.82703(1)	-1.58939(0)	2.90091(-2)	-2.26428(-4)
11	8.22737(4)	-3.13677(4)	5.10929(3)	-4.60917(2)	2.48726(1)	-8.02964(-1)	1.43604(-2)	-1.09772(-4)
12	1.13444(5)	-4.31547(4)	7.01286(3)	-6.31112(2)	3.39709(1)	-1.09376(0)	1.95058(-2)	-1.48650(-4)
13	1.01843(5)	-3.86748(4)	6.27350(3)	-5.63500(2)	3.02707(1)	-9.72559(-1)	1.73051(-2)	-1.31559(-4)
14	1.08377(5)	-4.11295(4)	6.66699(3)	-5.98385(2)	3.21177(1)	-1.03095(0)	1.83255(-2)	-1.39160(-4)

(b) Coefficients in equation (14)

Division	R_0	R_1	R_2	R_3	R_4	R_5	R_6	R_7
9	2.62274(5)	-1.05989(5)	1.83105(4)	-1.75301(3)	1.00440(2)	-3.44388(0)	6.54280(-2)	-5.31302(-4)
10	7.12464(4)	-2.85659(4)	4.89537(3)	-4.64869(2)	2.64146(1)	-8.97983(-1)	1.69096(-2)	-1.36054(-4)
11	8.04692(4)	-3.12290(4)	5.17513(3)	-4.74786(2)	2.60421(1)	-8.53945(-1)	1.54996(-2)	-1.20130(-4)
12	1.31662(5)	-5.02897(4)	8.20078(3)	-7.40207(2)	3.99385(1)	-1.28816(0)	2.29975(-2)	-1.75322(-4)
13	1.83427(5)	-6.93047(4)	1.11789(4)	-9.97990(2)	5.32574(1)	-1.69891(0)	2.99980(-2)	-2.26186(-4)
14	1.20645(5)	-4.57333(4)	7.40270(3)	-6.63405(2)	3.55496(1)	-1.13913(0)	2.02111(-2)	-1.53180(-4)

*Numeral A(k) should read as $A \times 10^k$.

TABLE 8.- COEFFICIENTS TO CALCULATE THE TRANSMITTANCE AND THE O_2 DISSOCIATION RATES IN METHOD SO(2)
FOR THE HEIGHT-DEPENDENT TEMPERATURE

(a) Coefficients in equation (13)								
Division	P_0	P_1	P_2	P_3	P_4	P_5	P_6	P_7
9	2.425470(5)*	-9.624982(4)	1.634189(4)	-1.538926(3)	8.681247(1)	-2.933657(0)	5.499110(-2)	-4.411116(-4)
10	9.669204(4)	-3.720173(4)	6.120147(3)	-5.581338(2)	3.047686(1)	-9.965949(-1)	1.807304(-2)	-1.402446(-4)
11	1.758494(5)	-6.642738(4)	1.071749(4)	-9.574185(2)	5.114708(1)	-1.634098(0)	2.891237(-2)	-2.185616(-4)
12	1.594939(5)	-6.022813(4)	9.714026(3)	-8.674938(2)	4.632826(1)	-1.479664(0)	2.617115(-2)	-1.977668(-4)
13	1.999395(5)	-7.509682(4)	1.204521(4)	-1.069549(3)	5.678393(1)	-1.802658(0)	3.168603(-2)	-2.379107(-4)
14	1.536738(5)	-5.782068(4)	9.291203(3)	-8.265891(2)	4.397255(1)	-1.398852(0)	2.464124(-2)	-1.854291(-4)

(b) Coefficients in equation (14)								
Division	R_0	R_1	R_2	R_3	R_4	R_5	R_6	R_7
9	2.513007(5)	-1.009141(5)	1.733542(4)	-1.651368(3)	9.420378(1)	-3.217900(0)	6.093978(-2)	-4.935429(-4)
10	-9.579851(4)	3.591625(4)	-5.737624(3)	5.060408(2)	-2.660443(1)	8.334936(-1)	-1.440281(-2)	1.058476(-4)
11	6.218042(4)	-2.412592(4)	3.998560(3)	-3.670430(2)	2.015139(1)	-6.616500(-1)	1.202909(-2)	-9.341187(-5)
12	1.845680(5)	-6.993932(4)	1.131505(4)	-1.013242(3)	5.423934(1)	-1.735661(0)	3.074329(-2)	-2.325326(-4)
13	2.492372(5)	-9.351094(4)	1.497706(4)	-1.327578(3)	7.034002(1)	-2.227787(0)	3.905472(-2)	-2.923659(-4)
14	1.554055(5)	-5.847188(4)	9.393681(3)	-8.354542(2)	4.442797(1)	-1.412750(0)	2.487460(-2)	-1.870930(-4)

*Numeral A(k) should read as $A \times 10^k$.

TABLE 9.- COMPARISON AMONG VARIOUS METHODS OF MEMORY SIZES NECESSARY FOR STORING THE COEFFICIENTS AND THE COMPUTATION TIME; THE LATTER IS SHOWN AS THE RATIO TO THE TIME IN SO(2)

Method	Hudson and Mahle (ref. 2)	Kockarts (ref. 3)			SO(1)	SO(2)
Division	Band-to-band	Band-to-band	10 Å	500 cm^{-1}	Band-to-band	50 Å
Memory size	5538	320	480	256	304	96
Computation time	~3.3[a]	~3.7	~5	~3	~3	1

[a]Needs additional time for calculating the necessary coefficients by interpolation.

TABLE 10.- PERCENTAGE DIFFERENCE OF THE RESULT CALCULATED BY METHOD SO(2) FROM THAT BY HUDSON-MAHLE ORIGINAL METHOD

Molecule	Temperature, °K	O_2 column density, cm^{-2}					
		10^{18}	10^{19}	10^{20}	10^{21}	10^{22}	10^{23}
		%	%	%	%	%	%
O_2	300	21.5	28.7	23.2	2.4	2.9	-2.7
	250	17.9	19.8	12.3	-2.5	1.3	-3.7
	200	13.0	11.5	4.3	-8.7	-3.4	10.5
	150	7.1	4.0	-3.1	-12.8	-2.4	12.8
	V.T.*	14.0	9.8	7.0	-6.0	-0.5	8.0
N_2O	300	-0.4	2.4	-0.3	-8.2	-4.0	-19.6
	250	-0.1	2.8	1.4	-3.3	6.0	-6.2
	200	-0.8	1.7	5.6	0.8	9.2	14.3
	150	0.3	3.5	4.5	4.8	20.1	10.6
	V.T.	-1.6	2.2	6.2	-5.1	0.6	9.8
HNO_3	300	-0.7	2.5	0.5	-7.6	-3.4	-19.0
	250	-0.4	2.8	1.9	-3.3	5.9	-6.0
	200	-1.1	1.6	6.0	0.1	8.3	13.9
	150	-0.1	3.4	4.5	3.5	18.6	9.9
	V.T.	-1.9	2.0	6.6	-4.9	0.5	9.5
HCl	300	1.3	1.8	-4.4	-10.8	-7.2	-22.9
	250	1.6	2.9	-1.0	-2.8	5.8	-8.4
	200	1.4	3.1	4.2	4.6	13.3	12.7
	150	2.3	5.0	5.9	12.4	26.4	11.9
	V.T.	0.6	3.9	4.7	-5.2	1.0	8.0
SO_2	300	-2.9	1.6	1.1	-8.1	-3.4	-16.5
	250	-2.7	1.6	1.8	-5.0	4.1	-5.4
	200	-3.6	-0.1	5.5	-2.6	4.8	12.2
	150	-2.5	1.8	3.1	-0.5	13.9	7.3
	V.T.	-4.3	0.2	6.1	-6.3	-1.3	8.5
H_2O	300	21.8	20.2	9.2	-0.3	-12.3	-42.6
	250	22.2	24.5	19.3	26.6	21.9	14.9
	200	22.5	27.7	30.1	59.4	63.9	22.4
	150	23.4	31.6	43.4	98.4	112.2	43.9
	V.T.	22.0	29.2	29.4	23.6	18.1	9.2
H_2O_2	300	-2.4	0.5	-1.5	-9.2	-3.6	-15.7
	250	-2.2	0.9	-0.0	-5.4	3.5	-5.3
	200	-2.9	-0.2	4.2	-2.1	4.1	11.4
	150	-1.8	1.8	2.9	1.1	13.3	6.1
	V.T.	-3.6	0.3	4.6	-6.7	-1.9	8.2

TABLE 10.- PERCENTAGE DIFFERENCE OF THE RESULT CALCULATED BY METHOD SO(2)
FROM THAT BY HUDSON-MAHLE ORIGINAL METHOD — CONCLUDED

Molecule	Temperature, °K	O_2 column density, cm^{-2}					
		10^{18}	10^{19}	10^{20}	10^{21}	10^{22}	10^{23}
		%	%	%	%	%	%
CO_2	300	5.0	6.3	-2.8	-12.3	-12.2	-28.0
	250	5.3	9.2	4.4	3.1	6.1	13.2
	200	5.1	11.4	12.6	19.7	22.6	8.6
	150	6.4	14.3	20.7	38.9	42.7	9.8
	V.T.	4.9	12.6	12.4	0.0	2.2	2.9
$CFCl_3$	300	-5.3	-3.7	-7.4	-12.3	-4.6	-18.3
	250	-5.0	-3.1	-5.2	-7.1	5.0	-5.8
	200	-5.4	-3.7	-0.9	-2.4	8.1	13.7
	150	-4.5	-2.0	-1.1	2.3	18.7	9.9
	V.T.	-6.1	-3.2	-0.4	-8.7	-0.3	9.4
CF_2Cl_2	300	-0.1	3.1	0.3	-8.9	-7.0	-23.9
	250	0.2	3.3	2.0	-2.9	5.9	-8.4
	200	-0.5	2.4	6.0	1.9	12.9	14.6
	150	0.6	3.9	5.0	6.8	25.4	13.6
	V.T.	-1.5	2.9	6.8	-5.2	1.1	8.9

[a]V.T. (variable temperature) indicates the height-dependent temperature.
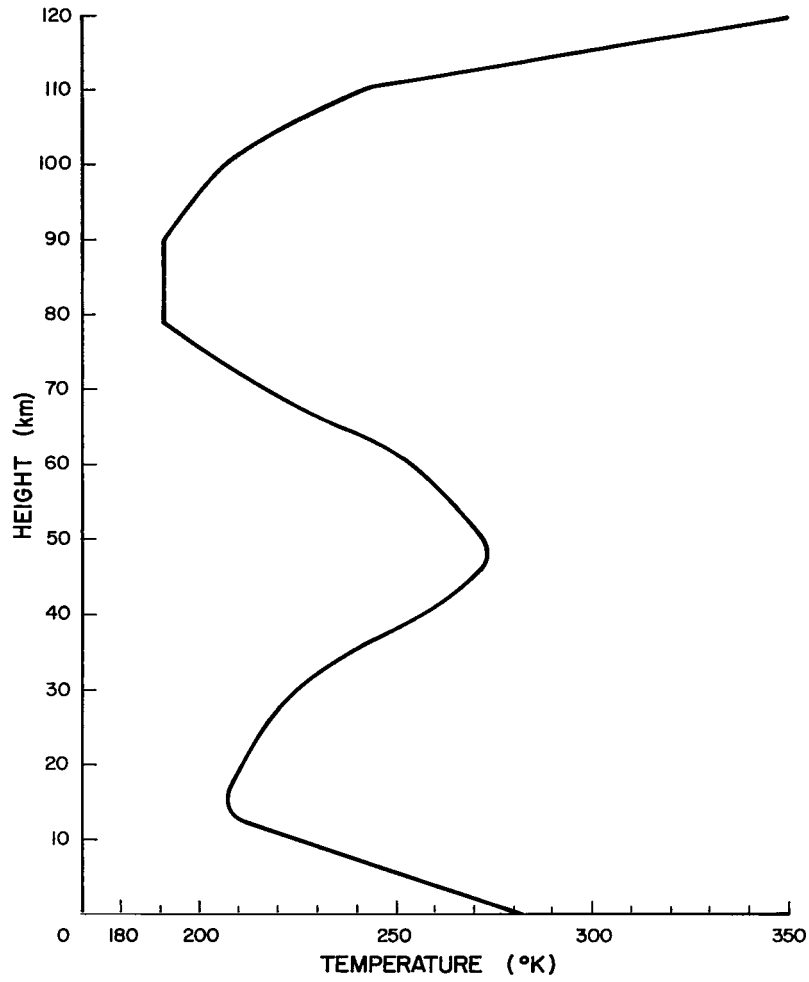
Figure 1.- The temperature profile used in the model calculations.
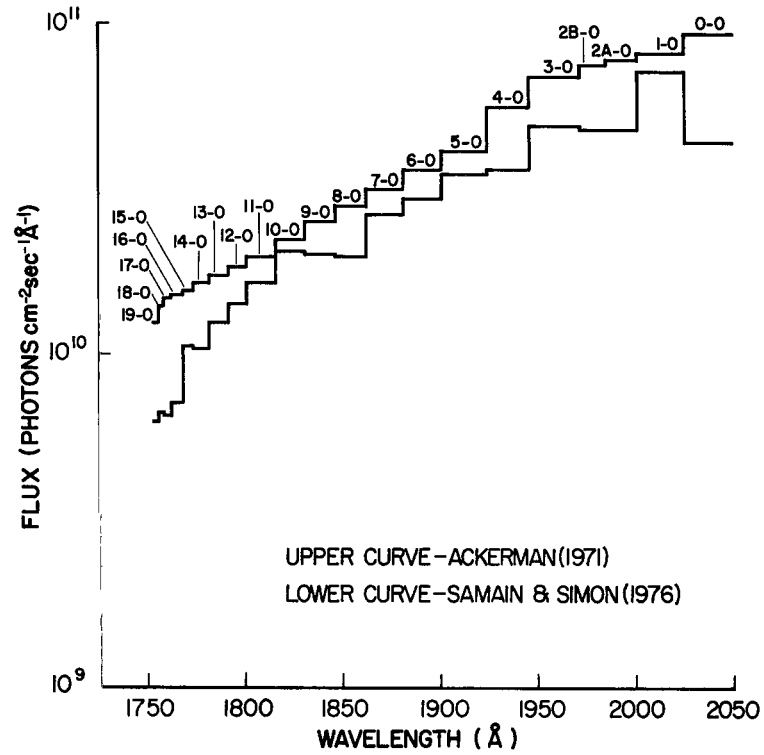
Figure 2.- Solar fluxes at each band of the Schumann-Runge band region.
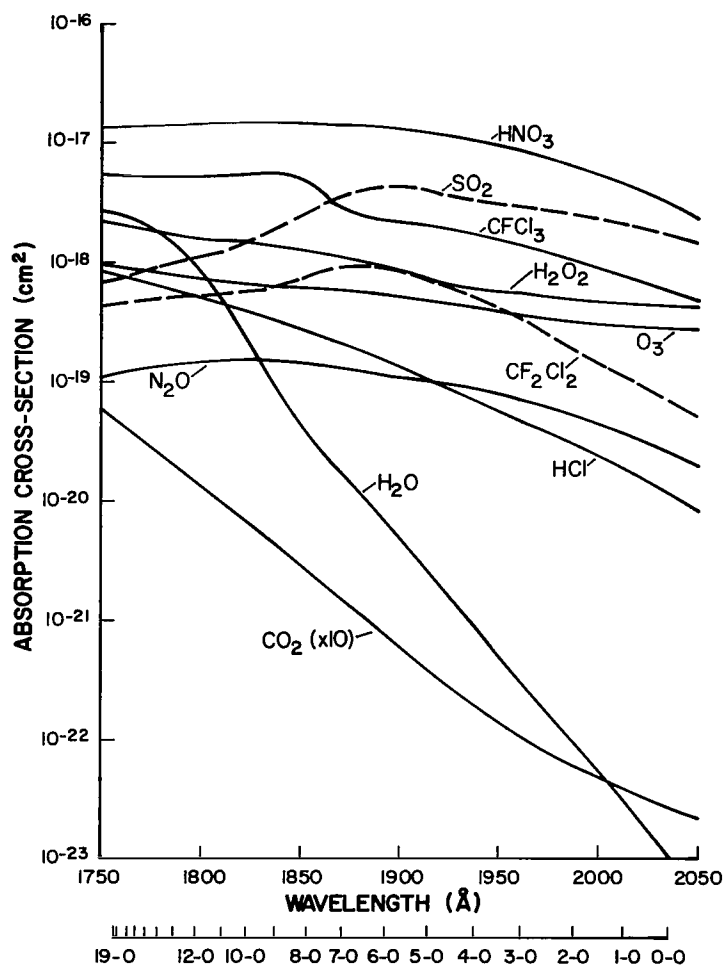
Figure 3.- Absorption cross sections of various molecules in the Schumann-Runge band system.

25
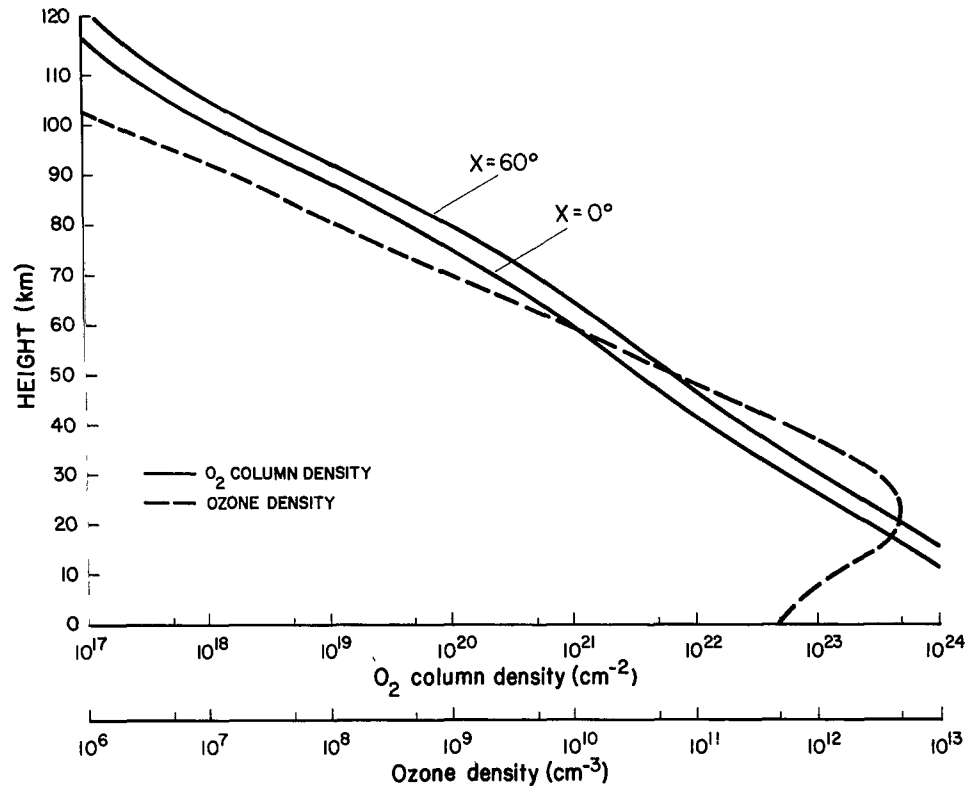
Figure 4.- An ozone density profile based on observations, and the relationship between the O_2 column density and the height of the atmosphere for the condition of overhead sun and a 60° solar incidence angle.
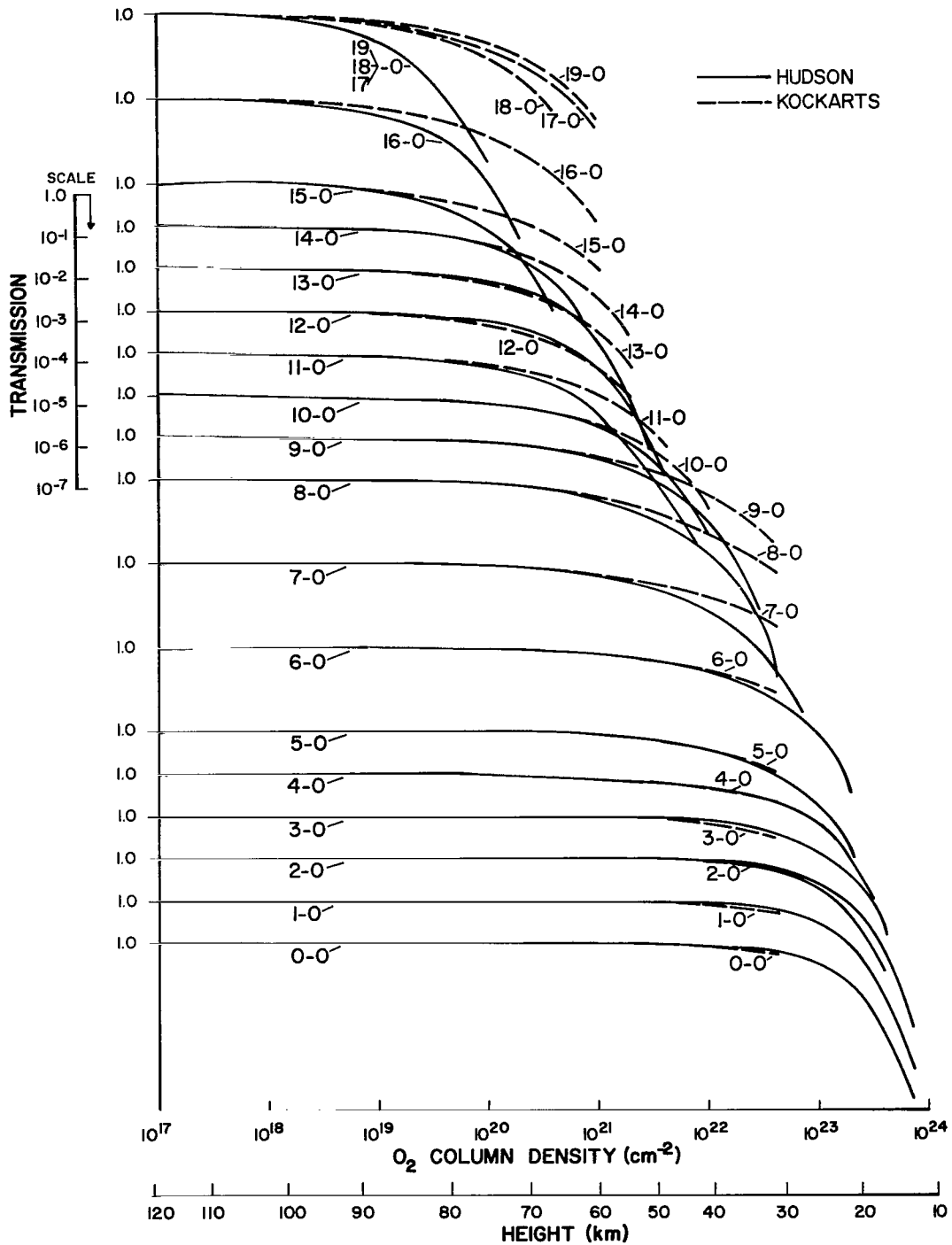
(a) Transmission at each band of the Schumann-Runge system.

Figure 5.- Comparison between the Hudson-Mahle and Kockarts methods.
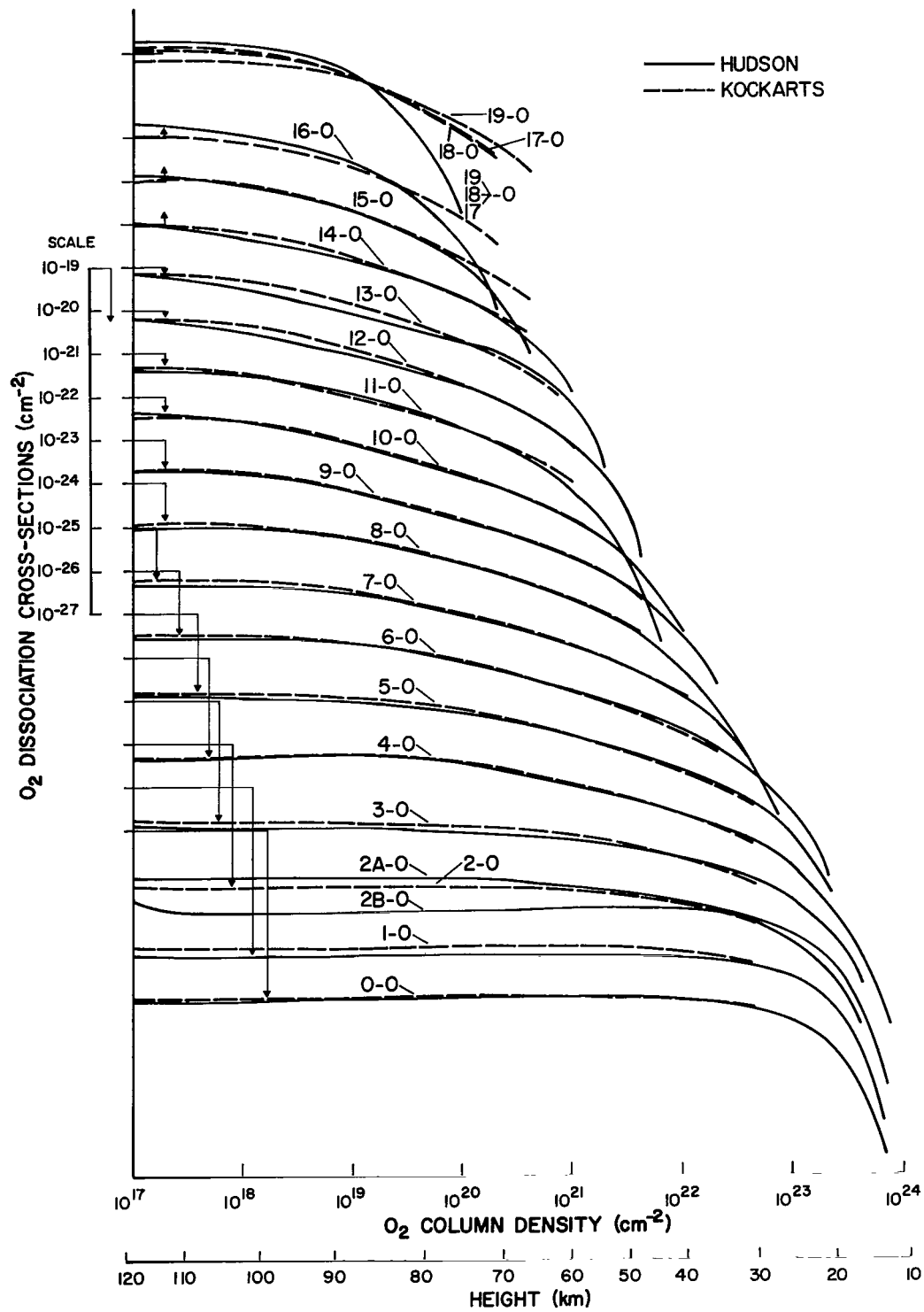
(b) O$_2$ predissociation coefficients at each Schumann-Runge band.

Figure 5.- Concluded.
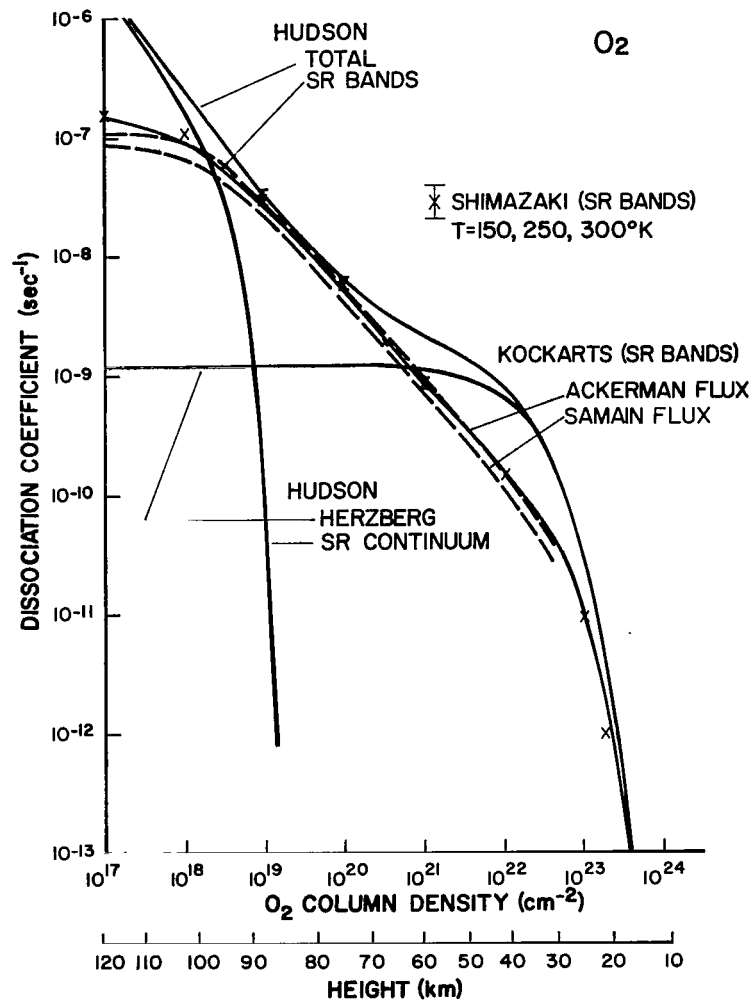
Figure 6.- Comparison of the O_2 dissociation coefficients calculated by various methods.
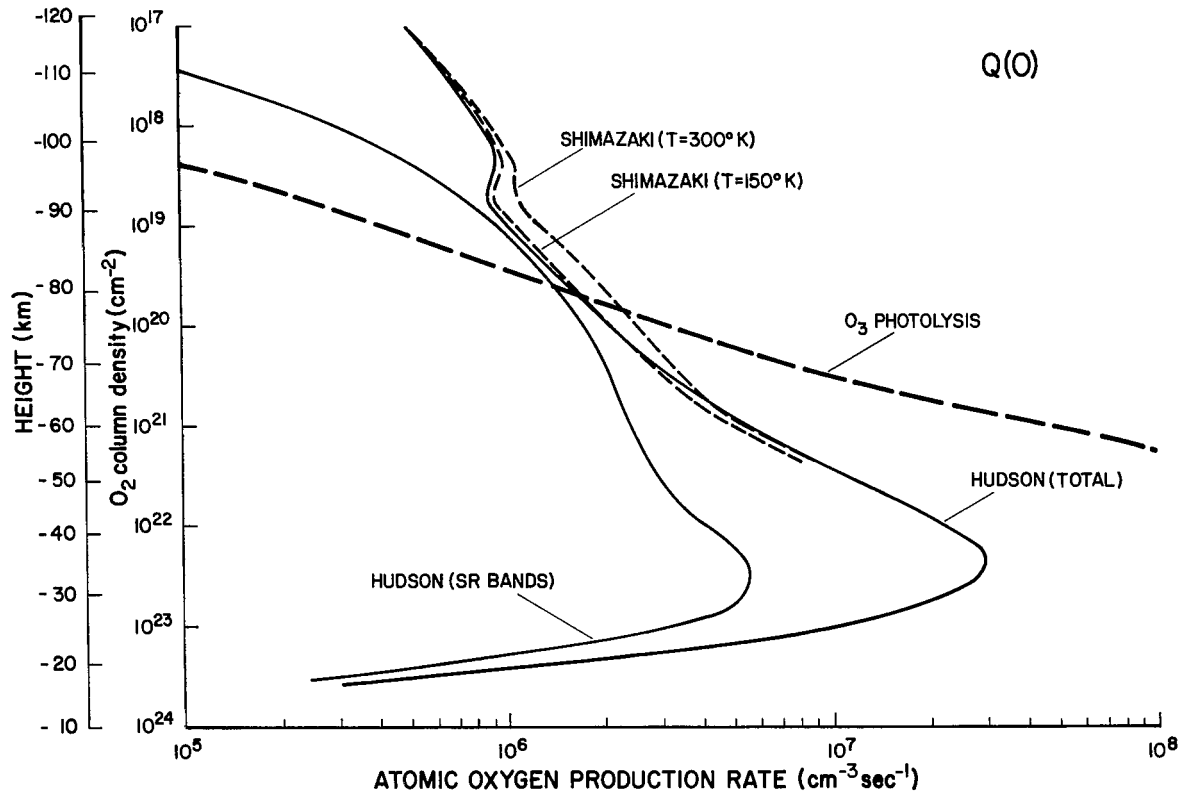
Figure 7.- Profiles of atomic oxygen production rate by O_2 and O_3 photolyses calculated by the Hudson-Mahle method and the Shimazaki-Ogawa method.
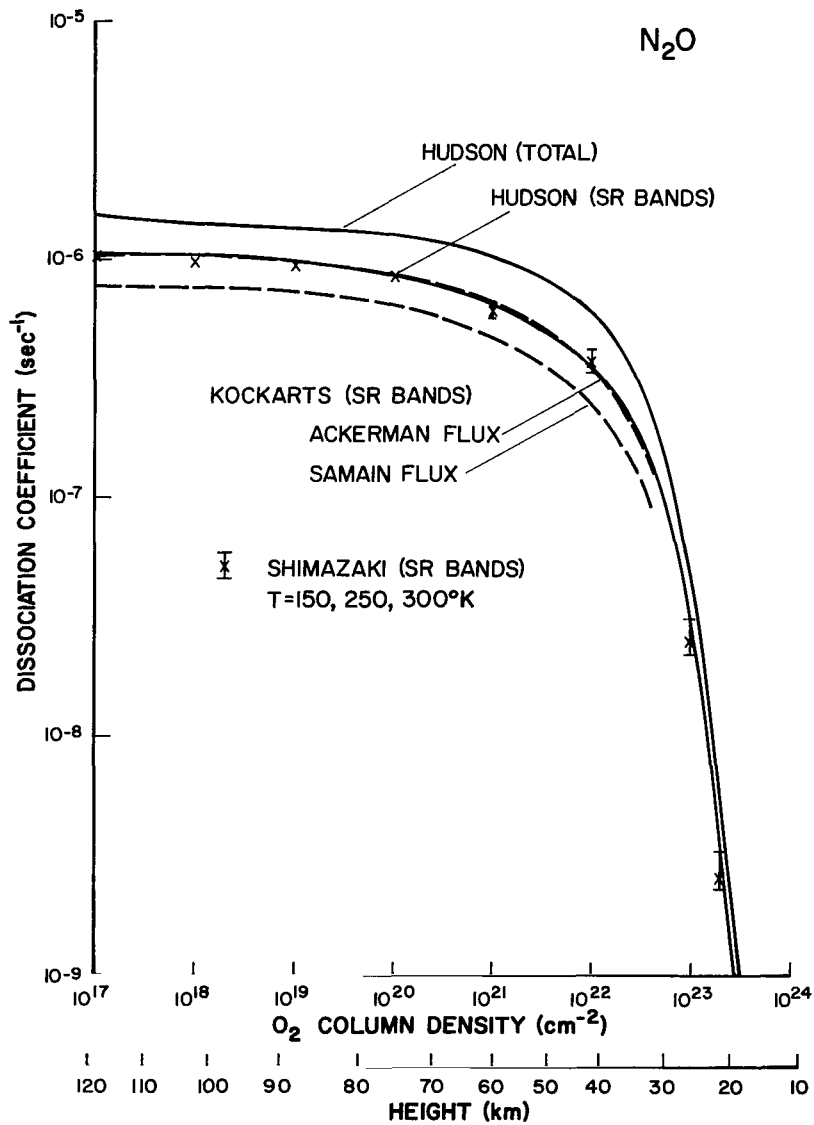
(a)   Dissociation coefficient for N_2O.

Figure 8.- Comparison of the dissociation coefficients calculated by various methods.
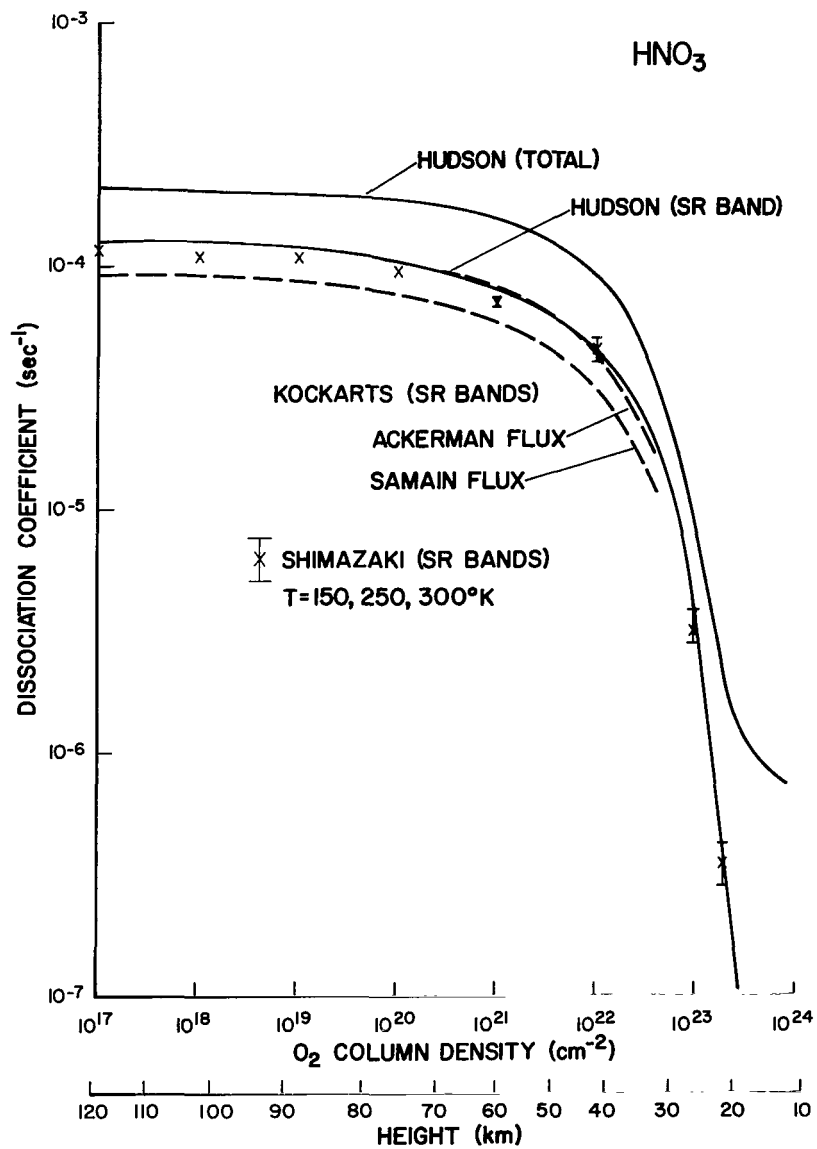
(b)   Dissociation coefficient for HNO_3.

Figure 8.- Continued.
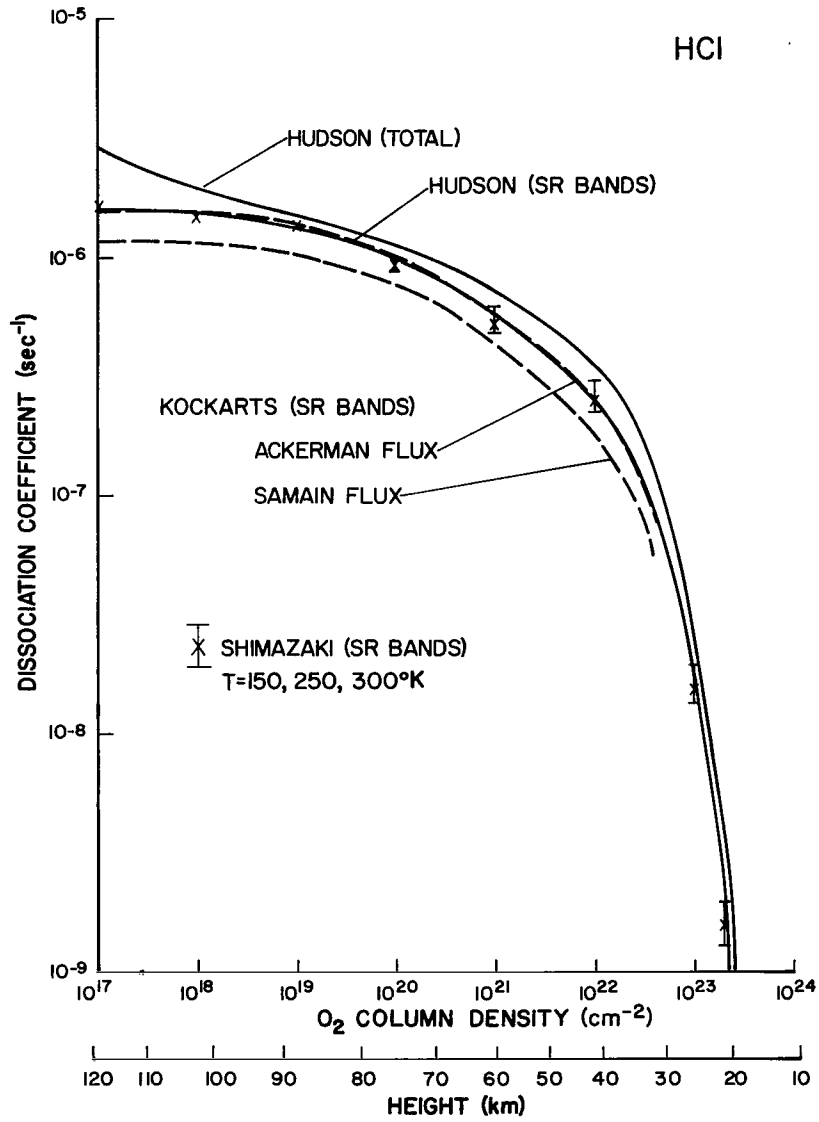
(c) Dissociation coefficient for HCl.

Figure 8.- Continued.
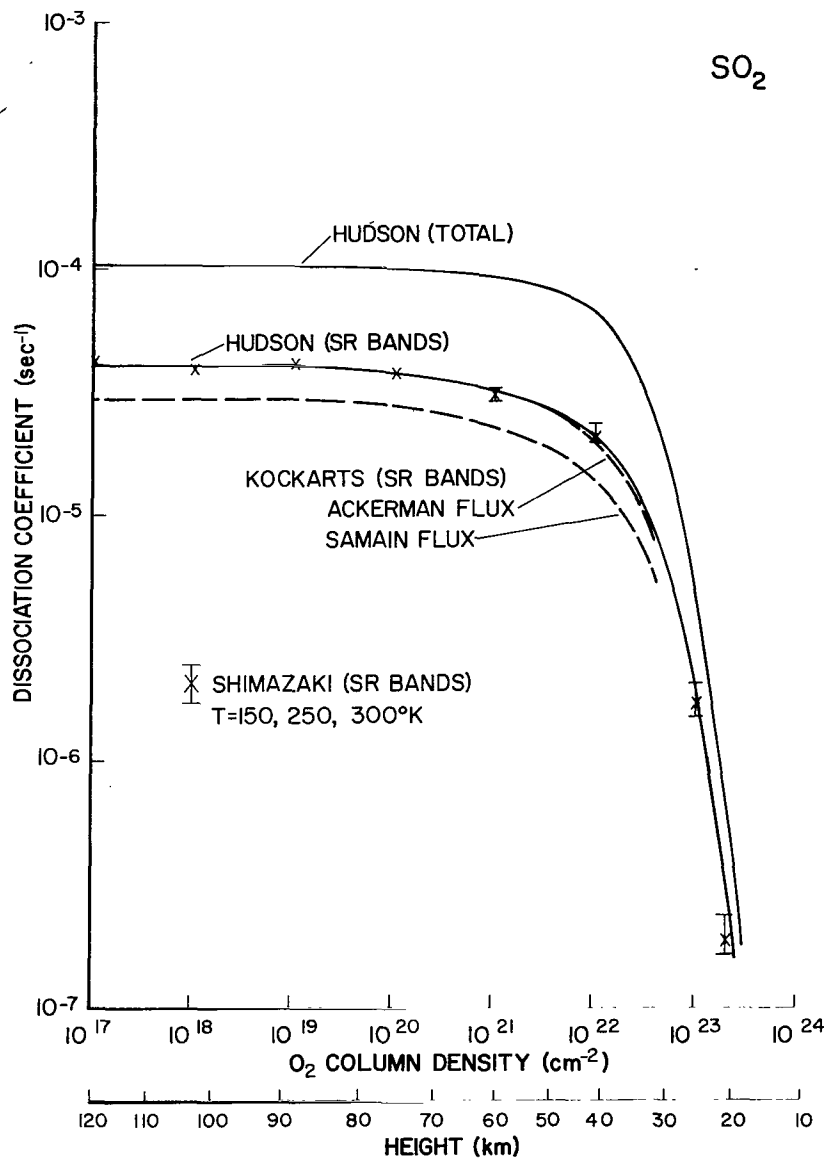
(d) Dissociation coefficient for SO_2.
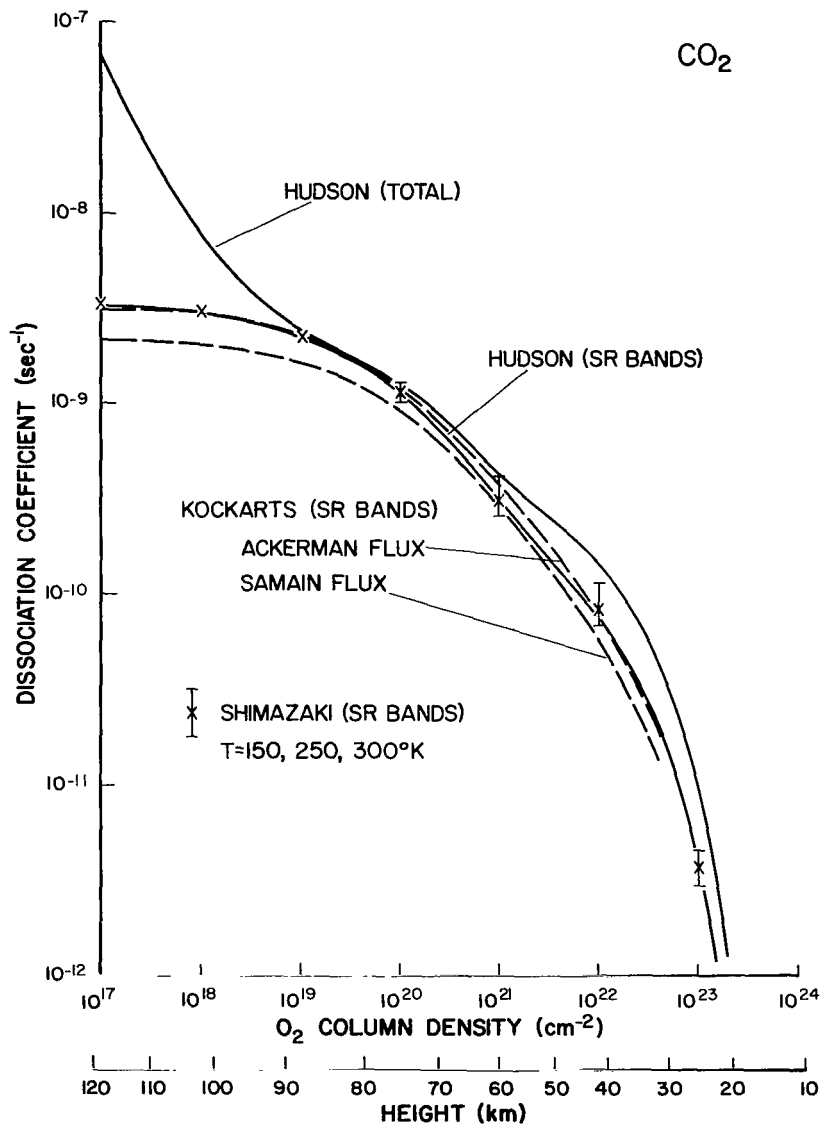
Figure 8.- Continued.
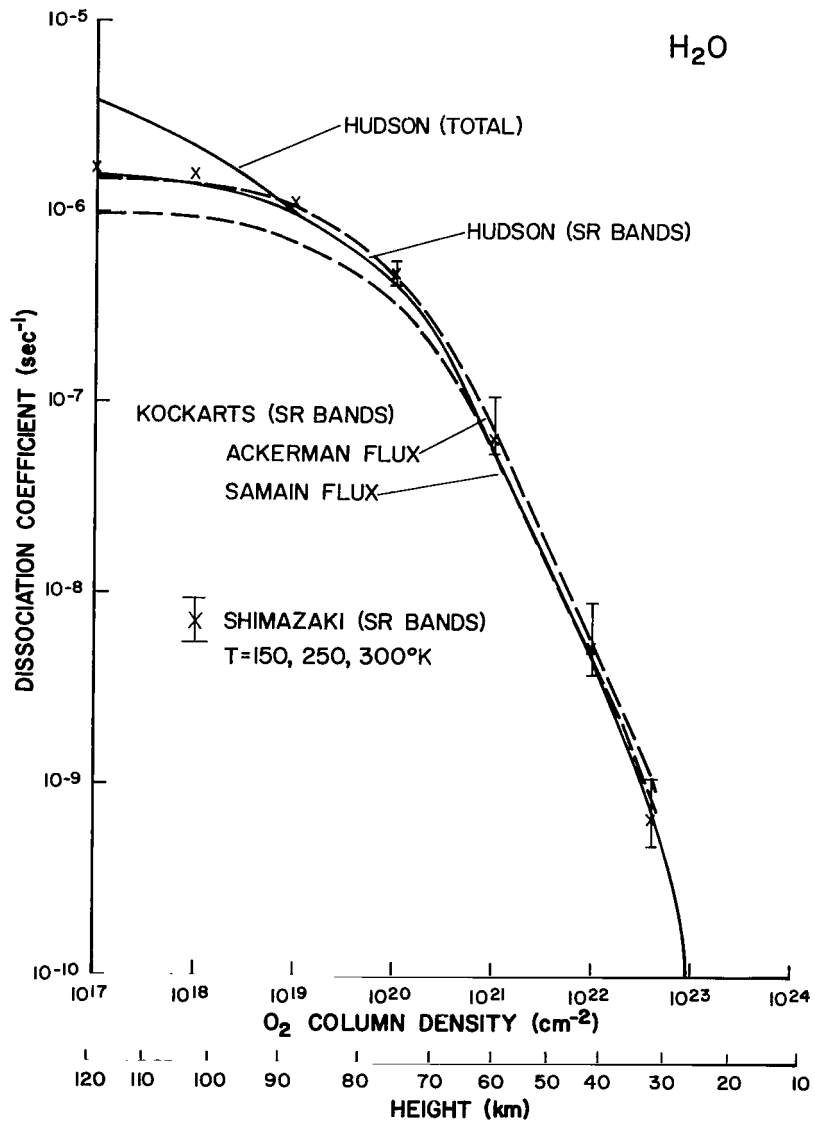
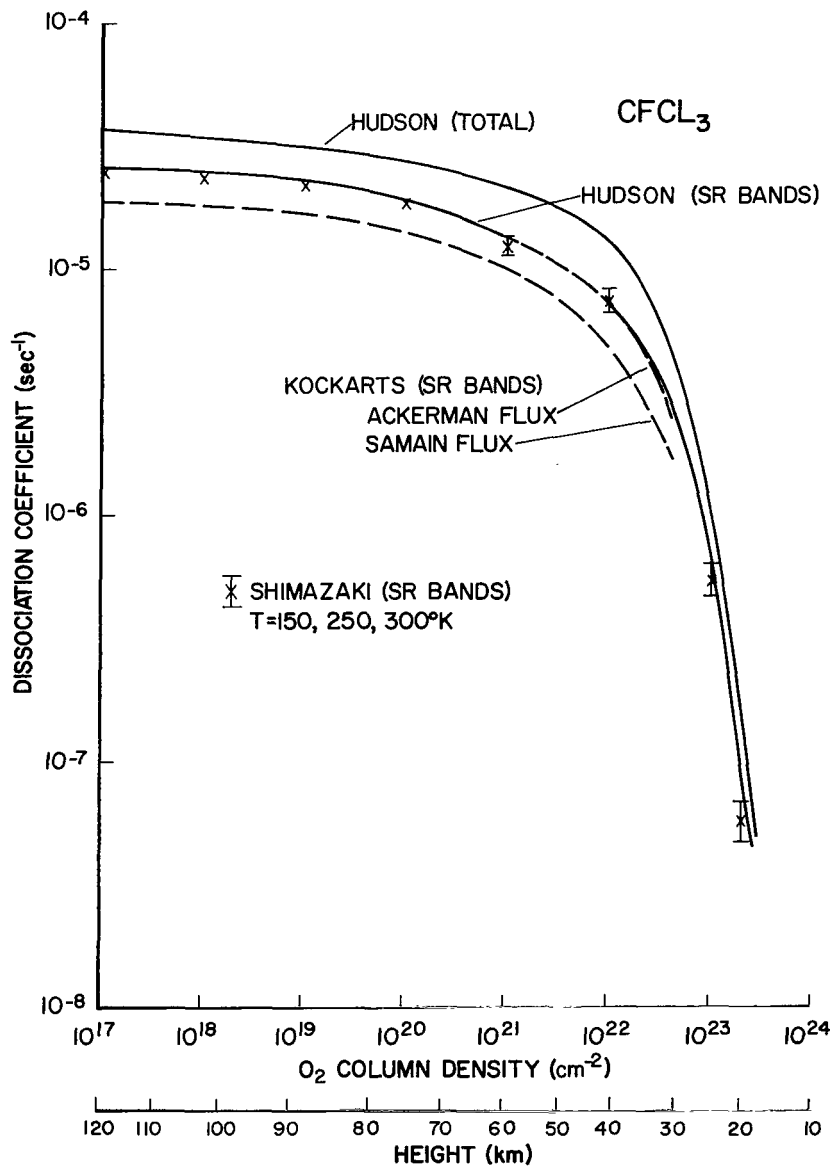(e) Dissociation coefficient for H_2O.

Figure 8.- Continued.
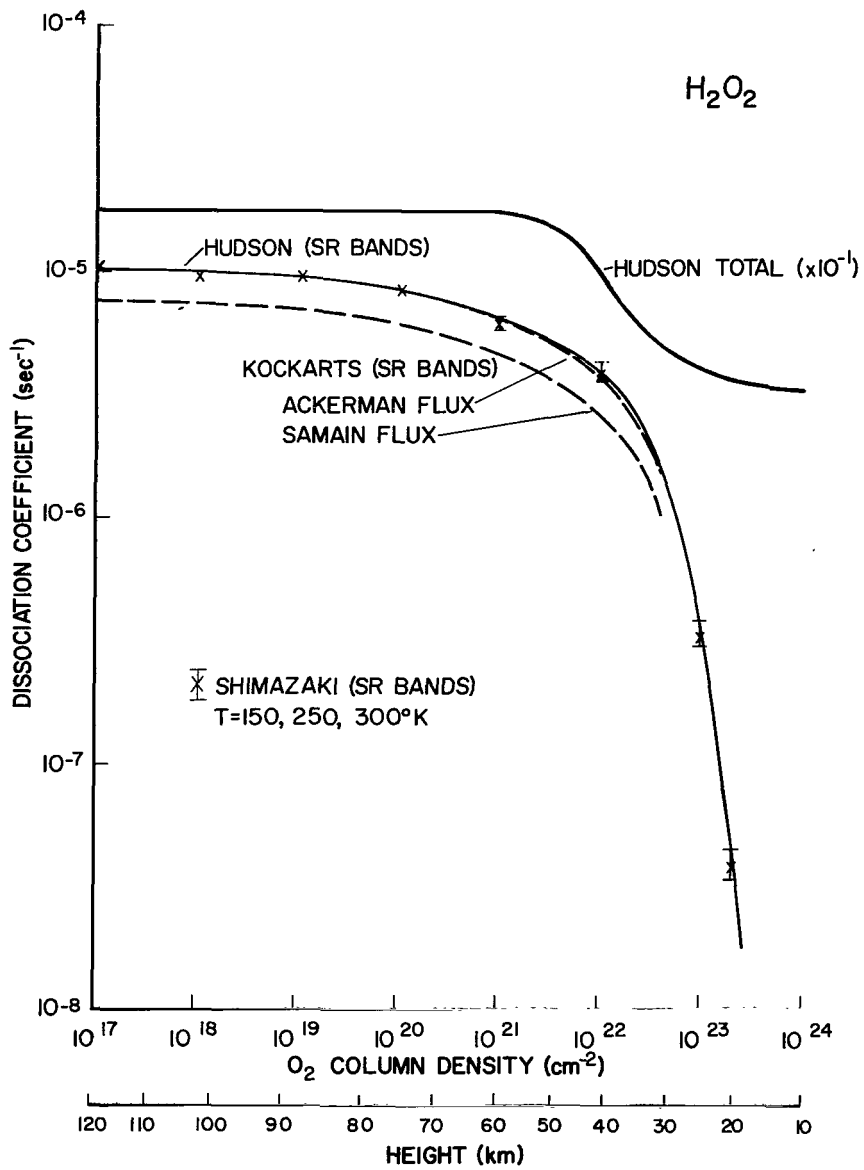
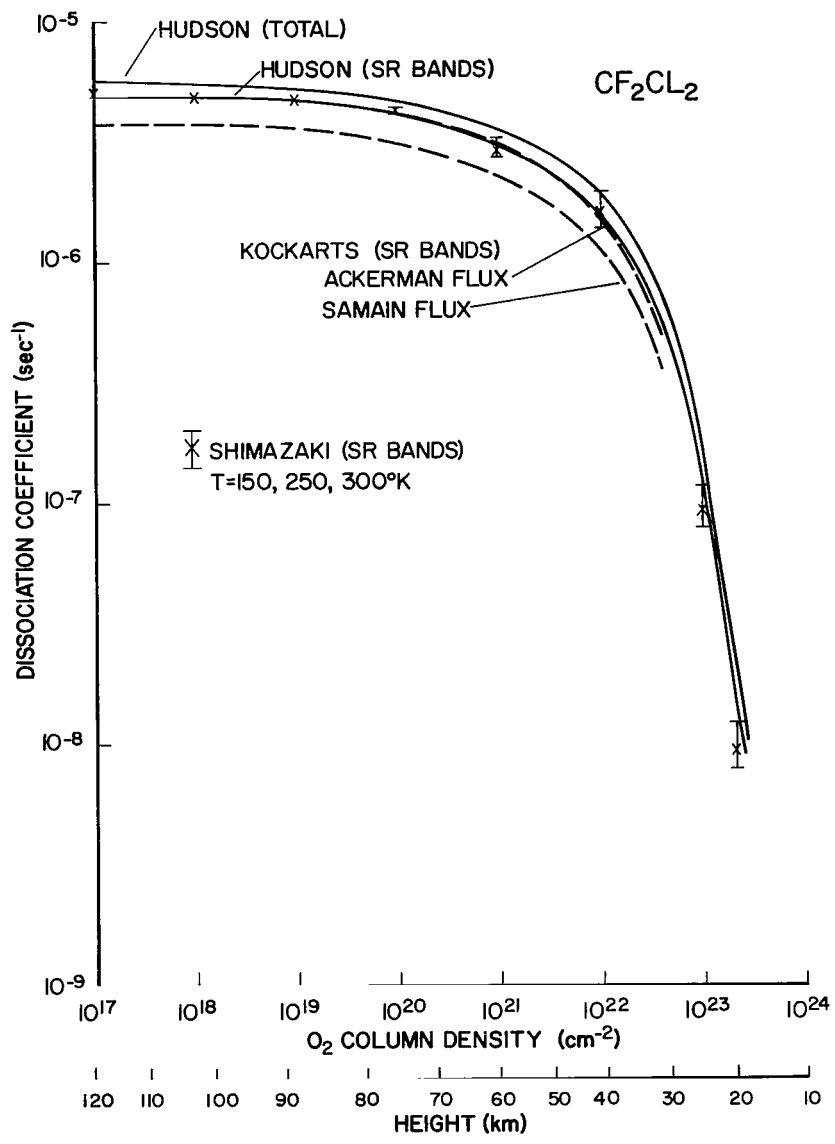(f) Dissociation coefficient for H_2O_2.

Figure 8.- Continued.

(g) Dissociation coefficient for CO_2.

Figure 8.- Continued.

(h) Dissociation coefficient for CFCl₃.

Figure 8.– Continued.

(i) Dissociation coefficient for CF_2Cl_2.

Figure 8.- Concluded.

233 001 C1 U   E 770318 S00903DS
DEPT OF THE AIR FORCE
AF WEAPONS LABORATORY
ATTN: TECHNICAL LIBRARY (SUL)
KIRTLAND AFB NM 87117

"The aeronautical and space activities of the United States shall be conducted so as to contribute . . . to the expansion of human knowledge of phenomena in the atmosphere and space. The Administration shall provide for the widest practicable and appropriate dissemination of information concerning its activities and the results thereof."
—NATIONAL AERONAUTICS AND SPACE ACT OF 1958

NASA SCIENTIFIC AND TECHNICAL PUBLICATIONS

TECHNICAL REPORTS: Scientific and technical information considered important, complete, and a lasting contribution to existing knowledge.

TECHNICAL NOTES: Information less broad in scope but nevertheless of importance as a contribution to existing knowledge.

TECHNICAL MEMORANDUMS: Information receiving limited distribution because of preliminary data, security classification, or other reasons. Also includes conference proceedings with either limited or unlimited distribution.

CONTRACTOR REPORTS: Scientific and technical information generated under a NASA contract or grant and considered an important contribution to existing knowledge.

TECHNICAL TRANSLATIONS: Information published in a foreign language considered to merit NASA distribution in English.

SPECIAL PUBLICATIONS: Information derived from or of value to NASA activities. Publications include final reports of major projects, monographs, data compilations, handbooks, sourcebooks, and special bibliographies.

TECHNOLOGY UTILIZATION PUBLICATIONS: Information on technology used by NASA that may be of particular interest in commercial and other non-aerospace applications. Publications include Tech Briefs, Technology Utilization Reports and Technology Surveys.

Details on the availability of these publications may be obtained from:

SCIENTIFIC AND TECHNICAL INFORMATION OFFICE

NATIONAL AERONAUTICS AND SPACE ADMINISTRATION
Washington, D.C. 20546